

Computation with Sequences of Assemblies in a Model of the Brain

Max Dabagia

School of Computer Science, Georgia Tech

MAXDABAGIA@GATECH.EDU

Christos H. Papadimitriou

Department of Computer Science, Columbia University

CHRISTOS@COLUMBIA.EDU

Santosh S. Vempala

School of Computer Science, Georgia Tech

VEMPALA@GATECH.EDU

Abstract

Even as machine learning exceeds human-level performance on many applications, the generality, robustness, and rapidity of the brain’s learning capabilities remain unmatched. How cognition arises from neural activity is *the* central open question in neuroscience, inextricable from the study of intelligence itself. A simple formal model of neural activity was proposed in [Papadimitriou et al. \(2020\)](#) and has been subsequently shown, through both mathematical proofs and simulations, to be capable of implementing certain basic cognitive operations via the creation and manipulation of assemblies of neurons. However, many intelligent behaviors rely on the ability to recognize, store, and manipulate temporal *sequences* of stimuli and memories (planning, language, navigation, to list a few). Here we show that, in the same model, the precedence of time can be captured naturally through synaptic weights and plasticity, and, as a result, a range of computations on *sequences* of assemblies can be carried out. In particular, repeated presentation of a sequence of stimuli leads to the memorization of the sequence through corresponding neural assemblies: Upon future presentation of any stimulus in the sequence, the corresponding assembly and its subsequent ones will be activated, one after the other, until the end of the sequence. If the stimulus sequence is presented to two brain areas simultaneously, a scaffolded representation is created, resulting in more efficient memorization and recall, in agreement with cognitive experiments. Finally, we show that any finite state machine can be learned in a similar way, through the presentation of appropriate patterns of sequences. Through an extension of this mechanism, the model can be shown to be capable of universal computation. We support our analysis with a number of experiments to probe the limits of learning in this model in key ways. Taken together, these results provide a concrete hypothesis for the basis of the brain’s remarkable abilities to compute and learn, with sequences playing a vital role.

Keywords: assemblies, neural network, neuroscience, plasticity, sequence learning, finite state machine

1. Introduction

How does the activity of individual neurons and synapses lead to higher-level cognitive functions? This is a central mystery in neuroscience which currently lacks an overarching theory. In [Papadimitriou et al. \(2020\)](#) a mathematical model of the brain was proposed in an attempt at such a theory. This neural model — which we call NEMO in this paper — entails brain areas, spiking neurons, random synapses, local inhibition, and plasticity (see the next subsection for a detailed description of NEMO). The dynamical system defined by NEMO has certain emergent attractors corresponding to *assemblies of neurons*; recall that an assembly is a stable set of highly interconnected neurons in an area, representing through their (near) simultaneous excitation a real-world object, episode,

or idea (Hebb, 1949; Harris et al., 2003; Buzsáki, 2019). There is a growing consensus in neuroscience that assemblies of neurons play an important role in the way the brain works (Buzsáki, 2010; Huyck and Passmore, 2013; Yuste, 2015; Eichenbaum, 2018). It was established in Papadimitriou et al. (2020) and subsequent research, through both mathematics and simulation, that certain elementary behaviors of assemblies arise in NEMO: projection, association, merge, among others. Moreover, through NEMO one can implement certain reasonably complex cognitive phenomena, including learning to classify well-separated classes of stimuli (Dabagia et al., 2022), and parsing natural language sentences (Mitropolsky et al., 2021).

Many of the brain’s remarkable capabilities rely on working with *sequences* (of stimuli, words, places, etc), with the human brain’s acumen for language being a particularly striking example. The capacity to memorize sequences is widely attested in cognitive neuroscience (Sugar and Moser, 2019; Bellmund et al., 2020). Experiments have documented the creation and activation of assemblies in sequence in the animal brain after training on tasks that involve sequential decisions (Dragoi and Buzsáki, 2006; Pastalkova et al., 2008; Dragoi and Tonegawa, 2011). Ikegaya et al. (2004) observed that precisely-timed patterns of activation across large groups of neurons in the mouse neocortex are frequently repeated, suggesting memorization, and moreover that these patterns are combined into higher-order sequences (i.e., sequences of sequences). In the hippocampi of rats performing a sequential decision-making task, Pastalkova et al. (2008) identified assembly sequences which predicted the decisions made. Across both navigational and memory tasks, the particular sequence which was exhibited depended closely on initial conditions and the structure of the task instance. In a further investigation by Dragoi and Tonegawa (2011), sequences of neurons that were observed during a novel experience also occurred in spontaneous activity during rest before the experience was initiated again, a phenomenon known as “preplay”. This finding suggests that the structure of sequence representations is largely determined by the intrinsic connectivity of the network.

Arguably, it is through sequences of stimuli and their representations that brains deal with the all-important concept of *time*. The question arises: Can NEMO capture this capability of the animal brain? In past work, NEMO did not have to deal explicitly with sequences or time. In the English parser implemented in Mitropolsky et al. (2021), the input sentence is presented sequentially, and the order of its words is not memorized by the device. In subsequent work on parsing Mitropolsky et al. (2022), the need to memorize subsequences of the input language became apparent in connection to the *center embedding* of sentences; however, no mechanism for this memorization was proposed.

In this paper, we demonstrate the emergent formation of sequences of assemblies in NEMO. When a brain area is stimulated by the same sequence of stimuli a handful of times, assemblies are reliably created, and the entire sequence will subsequently be recalled when only the beginning of the stimulus sequence is presented. Importantly, the underlying mechanism involves the capture of time precedence between sequences through the establishment, via plasticity, of high synaptic weights between stimuli representations, in the direction of time. Moreover, we demonstrate that involving additional brain areas during presentation (essentially forming a “scaffold” of interconnected assemblies) makes memorization faster and more robust, and more so if this new area already contains another memorized sequence. This provides theoretical support to experience: It is easier to memorize a sequence of stimuli when each stimulus is mentally associated by the subject with an element of an already memorized sequence — for example, a familiar tune, or the sequence of buildings next to the subject’s home.

We use these ideas to further show that, in NEMO, assemblies can be configured to simulate an arbitrary *finite state machine* (FSM, or *finite state automaton*). Recall that FSMs are simple computational devices capable of recognizing and generating the class of sequential patterns known as *regular languages* (Sipser, 1996). Moreover, we show that this configuration can be learned quickly by presenting sequences of stimuli corresponding to state transitions; this captures the brain’s ability to learn *algorithms* involving sequences. The implementation and learning of FSMs relies crucially on one last feature of NEMO, namely *long-range interneurons* (LRIs). These are neural populations extrinsic to the brain areas of NEMO, which can be recruited by assemblies in adjacent areas, and whose function is to inhibit or disinhibit remote brain areas to achieve synchrony and control of the computation (Sik et al., 1995; Jinno et al., 2007; Zhang et al., 2014). There is evidence in the literature Roux and Buzsáki (2015) that LRIs are essential for the onset of γ oscillations, often considered coterminous with brain computation.

One interesting byproduct of the mechanism for implementing and learning FSMs is a simple demonstration that NEMO is *Turing complete*. In other words, NEMO with LRIs constitutes a hardware language capable of implementing any computation, within the constraints imposed by the parameters of the model. This is rather significant for a mathematical model that has the ambition to capture a large part of human cognition. The original exposition of NEMO in Papadimitriou et al. (2020) did contain an argument of Turing-completeness as well; however, that proof relies on a biologically implausible computer-like program, with loops, conditional statements, and variables corresponding to assemblies. The Turing completeness argument in the present paper is carried out strictly within NEMO, and the required program is implemented with LRIs, yielding an entirely hardware-based general computer, consistent with neurobiological principles.

1.1. The Neural Model

We next describe in detail NEMO, the mathematical model of the brain we consider here. The essential ingredients are a weighted, directed, random graph, along with simple mechanisms for determining which neurons fire (*k*-winners-take-all) and adjusting the weights (Hebbian plasticity and homeostasis).

Brain areas. The *brain* consists of a finite number of *brain areas*. A brain area is a set of n excitatory neurons, connected internally by directed random edges (synapses), each present independently with probability p . Two brain areas A and B may be connected to each with edges in one direction (e.g., A to B) — or possibly in both directions — by a *fiber*. Fibers are directed bipartite random graphs; that is, if there is a fiber from A to B , then for each pair of excitatory neurons (i, j) where i is in A and j is in B , there is a synapse from i to j with probability p , independently of all other possible synapses. All synapses have *weights*, assumed to be initially one. An *input* (or *sensory*) area is a set of excitatory neurons, subsets of which are activated by external stimuli (e.g., the output of a sensory pathway, or the memory system) and excite brain areas it is connected to. (Fibers only go from sensory areas to other brain areas, not vice versa.)

The dynamical system. We assume that computation proceeds in discrete time steps. At each step, for each neuron its total synaptic input is determined by summing up the current weights of incoming connections from neighbors which fired on the previous time step. For each brain area, *only the k neurons with the highest total input fire at each step* (with ties broken randomly). This is an important part of the model, capturing local inhibition and the area’s inhibitory/excitatory

balance. Synapse weights, both within and between areas, are nonnegative and governed by Hebbian plasticity with parameter $\beta > 0$, so that each time j fires immediately after i fires, the weight of the synapse from i to j increases by a multiplicative factor of $1 + \beta$. In mathematical notation, at time t , let $x_A(t)$ be the set of neurons in area A , $W_A(t)$ be the recurrent weight matrix for area A , $W_{B,A}(t)$ the weight matrix from area B to area A , and $I_A(t)$ the inhibitory signal for area A . Then we have

$$\begin{aligned} x_A(t+1) &\leftarrow I_A(t) \cdot k\text{-cap} \left(\sum_B W_{B,A}(t) x_B(t) \right) \\ W_A(t+1) &\leftarrow W_A(t) + \beta (x_A(t+1) x_A(t)^\top) \odot W_A(t) \\ W_{B,A}(t+1) &\leftarrow W_{B,A}(t) + \beta (x_A(t+1) x_B(t)^\top) \odot W_{B,A}(t) \end{aligned}$$

where \odot is element-wise multiplication, and the function $k\text{-cap}$ maps a vector to the indicator vector of its k largest components (with ties broken randomly).

Long-range interneurons. We assume that any brain area A can be inhibited — that is, no excitatory neuron in A can fire — by the activation of a designated population of inhibitory neurons, I_A . The activity of I_A can in turn be suppressed by the firing of a group of *disinhibitory* neurons D_A , which receive input from other brain areas. We assume that these two types of interneurons integrate much more quickly than excitatory neurons — as is generally accepted (Cruikshank et al., 2007; Zhou and Hablitz, 1998) — and as a result these inhibition and disinhibition actions can be thought of happening instantaneously.

1.2. Related work

The NEMO model is distinguished from other general theories of neuronal coordination by its bottom-up approach to the problem: It consists only of tractable abstractions of well-understood biological mechanisms, which can be shown to yield interesting behavior. Among other such theories, the neuroidal model presented by Valiant (2000a,b); Feldman and Valiant (2009) is powerful but demands neurons and synapses capable of arbitrary state changes, while attempts to translate the success of deep learning via gradient descent into the brain (Lillicrap et al., 2016; Sacramento et al., 2017; Guerguiev et al., 2017; Sacramento et al., 2018; Whittington and Bogacz, 2019; Lillicrap et al., 2020) rely on hypothetical feedback connections and exceedingly precise coordination.

Specifically in regard to memorizing and reproducing sequences, there are several other approaches which vary in biological fidelity and corresponding limitations. Eliasmith et al. (2012) is a biologically-plausible model of the entire brain which exhibits sequence memorization and prediction (along with other more complex cognitive tasks), but the mechanisms for doing so are complex and engineered, rather than emerging from simple dynamics. The model of Cui et al. (2016) is able to memorize and predict sequences in much the same fashion that we present here, using Hebbian plasticity and k -winners-take-all to abstract inhibition, but requires more sophisticated compartmental neurons and columnar organization. Lastly, the Tolman-Eichenbaum machine (Whittington et al., 2020) is an abstraction of the hippocampus which can memorize sequences (along with more general structured sets of stimuli), but its encoding and mechanisms are simply assumed and it is trained with gradient descent. In comparison with these, NEMO is distinguished by (i) the simplicity and biological fidelity of its mechanisms and (ii) the fact that its interesting behavior is emergent, with minimal “engineering”.

A model very closely related to NEMO and called *the assembly calculus (AC)* was described in [Papadimitriou et al. \(2020\)](#), where it was shown that it is Turing complete. The simulation of a Turing machine was accomplished using what amounts to a stored *program* of control commands, entailing variables, conditional statements, and loops, including commands needed for inhibiting and disinhibiting brain areas. A key contribution of this paper is that we eliminate such programs and use biologically plausible LRIs with similar consequences. As a result, our simulation is entirely self-contained, and driven only by the presentation of stimuli — the higher-level connectivity of brain areas and interneurons can implement the general architecture of a Turing machine (i.e. a long tape of symbols and a tape head which keeps track of the current state and reads and writes symbols on the tape), while the weights of connections between neurons store the actual symbols on the tape and the state transitions of the tape head.

Sequences of assemblies in neuroscience. There is a large body of experimental evidence from neuroscience indicating that neural representations of temporally-structured patterns of stimuli often preserve that structure. The assemblies hypothesis goes a step further: these neural representations ought not to arise only in response to the sequence of stimuli, but should also be generated internally by the network, for example by playing out the entire sequence of neural responses in response to only a fragment of the entire pattern of stimuli. Here we recount certain inspiring experimental results which support this view. In [Dragoi and Buzsáki \(2006\)](#), neurons in the hippocampi of rats running a linear maze were recorded, and the pairwise temporal correlations of their spikes were computed. These correlations were significantly larger than predicted by the model where neurons simply fire in response to where the animal currently is, suggesting that neurons which fire in response to one location of the maze become linked with those in nearby locations. [Pastalkova et al. \(2008\)](#) trained rats to alternate between two paths of a maze, with a delay period between each run, while again recording from the hippocampus throughout. They found that the activity during the delay period was a strong predictor of which path the rat would take, even on error runs (where the animal failed to alternate between paths correctly). As the environmental context was identical during these delay periods, this points to internal generation of these neural responses. Finally, [Dragoi and Tonegawa \(2011\)](#) recorded from the hippocampi of mice during periods of sleep and exploration of an unfamiliar maze, and found that the sequences of firing which occurred during exploration matched those that occurred during prior sleep periods. These sequences were active before the animal even saw the novel maze, which suggests that particular temporal patterns of neural activity arise spontaneously, and these patterns are later recruited to represent environmental stimuli. Although the sequences of firings which arise in our model need not occur spontaneously before the first presentation of the stimulus sequence, they do rely crucially on internal connectivity, and by repeated presentation of the stimulus sequence become linked together to reinforce the replay of the sequence.

2. Computation with sequences of assemblies

2.1. Sequence memorization

We begin with *sequence projection*, where a sequence of assemblies from one area is projected to another area. The most natural way to project a sequence from one area to another is to simply activate, in the first area, the assemblies for each element of the sequence, one after the other in the given order. Assuming that there is a fiber connecting the first area to the second, and the second

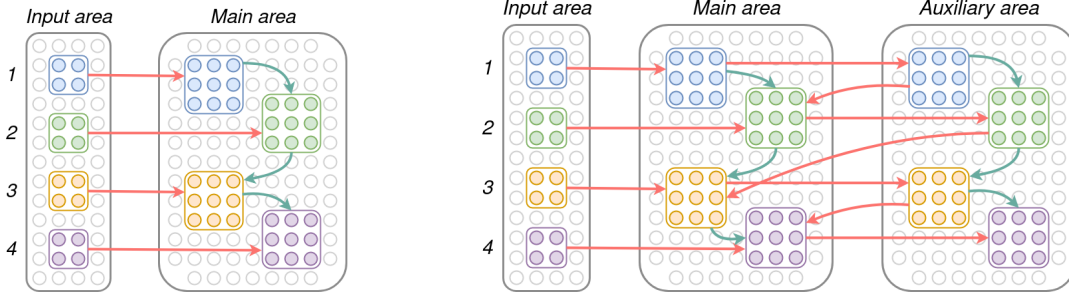


Figure 1: Left: Simple copy of a sequence of assemblies. When a sequence is played a few times in one area, a corresponding sequence of assemblies is formed in an adjacent area, and will subsequently be recalled when only the beginning of the sequence is presented in the input area. Right: When the area with the copied sequence is also allowed to send and receive input to/from an auxiliary area, a “scaffolded” sequence of assemblies is formed across the two areas, leading to faster, more reliable memorization.

area is disinhibited, one would hope that this would result in the creation of a set of corresponding assemblies in the target area, so that activating any newly created assembly results in the sequential activation of the rest of the sequence of new assemblies. This is the essence of our first finding, stated below with quantitative bounds on plasticity and the other parameters.

Theorem 1 (Simple sequence copy) *Suppose that area A receives input from area S . Let S_1, \dots, S_L be a sequence of subsets of k neurons from S , with $L \leq n/2k$, and $|S_\sigma \cap S_{\sigma'}| \leq \Delta$ for all $\sigma \neq \sigma' \in \{1, 2, \dots, L\}$, and Δ a positive integer. Suppose this sequence is presented T times (with each presentation beginning from rest) with area A disinhibited, forming a sequence of caps $A_1(t), \dots, A_L(t)$ in area A on round $t \leq T$. After each round, homeostasis is applied, so that each neuron’s incoming weights sum to 1. Then for*

$$kp \geq 3 \ln n, \quad \Delta \leq \frac{k}{(2 \ln n)^2}, \quad \beta \leq \frac{\ln \frac{n}{2kL}}{2(\max\{\Delta p, 6 \ln n\})^2}, \quad T \geq \frac{1}{\beta \ln(n/k)}$$

when any S_i fires once in the input area, and A is allowed to fire $L - i + 1$ times, the resulting sequence of caps $\hat{A}_i, \dots, \hat{A}_L$, satisfies

$$\frac{\mathbb{E}[|\hat{A}_j \cap A_j(1)|]}{k} \geq 1 - \left(\frac{k}{n}\right)^{2\beta T}$$

for all $j \geq i$. In particular, for

$$T \geq \frac{1}{2\beta} \sqrt{\frac{\ln(nL)}{\ln(n/k)}}$$

w.h.p. we get perfect recall of the entire sequence after projection.

In other words, following T rounds of rehearsal, subsequent presentation of any input assembly in the sequence results in the activation of the corresponding assembly and the rest of the sequence in the target area. We note that the number of presentations needed grows inversely with the plasticity, and crucially, the plasticity cannot be too high.

Memorization with a scaffold. A well-known phenomenon in cognitive science is that memorization is easier by creating associations such as mnemonics. For sequences, learning one sequence by associating with another sequence, element by element (e.g., learning the alphabet to a tune), helps with retention and recall. We consider a very simple form of this: when projecting a sequence, we create two copies of the sequence that “scaffold” each other. Remarkably, this leads to provably better recall of the sequence with about half as many training rounds as simple sequence projection.

Theorem 2 (Scaffold sequence copy) *Suppose that areas A and B are connected to each other, and only A receives input from area S . Consider a sequence S_1, \dots, S_L of sets of k neurons in area S , for $L \leq n/2k$, which satisfy $|S_\sigma \cap S_{\sigma'}| \leq \Delta$ for all $\sigma \neq \sigma'$. Suppose this sequence is presented T times (with each beginning from rest) with areas A and B disinhibited, to form a sequence of caps $A_1(t), \dots, A_L(t)$ within A , and $B_1(t), \dots, B_L(t)$ within B on round t . After each round, homeostasis is applied, so that each neuron’s incoming weights sum to 1. Then for*

$$kp \geq 3 \ln n, \quad \Delta \leq \frac{k}{(2 \ln n)^2}, \quad \beta \leq \frac{\ln \frac{n}{2kL}}{2(\max\{\Delta p, 6 \ln n\})^2}, \quad T \geq \frac{1}{\beta \ln(n/k)}$$

when any S_i fires once (for $1 \leq i \leq L$), and A and B are allowed to fire $L - i + 1$ times to form a sequence of caps $\hat{A}_1, \dots, \hat{A}_L$ and $\hat{B}_1, \dots, \hat{B}_L$, we will have

$$\frac{\mathbb{E}[|\hat{A}_j \cap A_j(1)|]}{k}, \frac{\mathbb{E}[|\hat{B}_j \cap B_j(1)|]}{k} \geq 1 - \left(\frac{k}{n}\right)^{4\beta T}$$

for any $j \geq i$. In particular, for

$$T \geq \frac{1}{4\beta} \sqrt{\frac{\ln(nL)}{\ln(n/k)}}$$

w.h.p. we get perfect recall of the entire sequence in both areas A and B .

We note that the bound on the number of training rounds is a factor of two smaller here compared to simple sequence projection (Figure 6).

2.2. (Dis)inhibition with interneurons

Interneurons serve to inhibit and disinhibit areas. The lemma below shows that by connecting D_A to B and D_B to A , we get alternate firing of the two areas A and B . More precisely, the firing of a cap in area B causes D_A to fire, which causes I_A to cease firing, which allows a cap in A to fire in response to input from S and B (see Figure 2).

Lemma 3 (Alternation) *Let D_A receive input from B and D_B receive input from A , with A and B connected to each other and both receiving input from S . For any sequence of inputs S_1, S_2, \dots in the input area, where D_A and I_B are initially firing, the resulting sequence of activations S'_1, S'_2, \dots satisfies $S'_\sigma \subseteq A$ for σ odd and $S'_\sigma \subseteq B$ for σ even.*

Proof By induction on σ . For the base case $\sigma = 1$, as I_A is not firing initially and I_B is, only neurons in A will fire. So, $S'_1 \subseteq A$. More generally assume the claim holds for all $\sigma' < \sigma$. If σ is even, then $S'_{\sigma-1} \subseteq A$ and $S'_{\sigma-2} \subseteq B$ so D_B and I_A fired on the previous round. Hence, B is

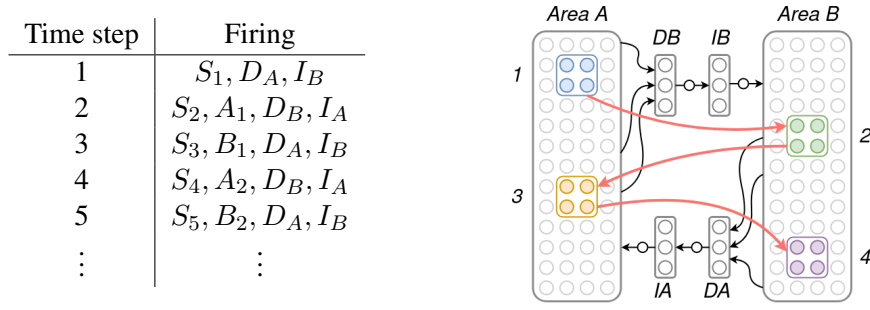


Figure 2: An example sequence of firings with interneurons. The table on the left shows the sets of neurons firing simultaneously on each round; on the right is the architecture of the network.

disinhibited and A is inhibited, so $S'_\sigma \subseteq B$. If σ is odd, then $S'_{\sigma-1} \subseteq B$ and $S'_{\sigma-2} \subseteq A$, so D_A and I_B fired on the previous round. Hence, A is disinhibited and A is inhibited, so $S'_\sigma \subseteq A$. ■

We will make extensive use of this property in the next section.

2.3. Learning finite state machines

Here we demonstrate that NEMO is powerful enough to simulate an arbitrary finite state machine (FSM). In fact, an FSM is learned — that is, memorized — simply by presenting all valid transitions between states in the FSM.

Finite state machines. A finite state machine (FSM) is a tuple $F = (Q, \Sigma, q_0, q_A, q_R, \delta)$, where Q is a set of states, Σ is a finite input alphabet, $q_0 \in Q$ is the initial state, and $\delta: Q \times \Sigma \rightarrow Q$ is the transition function, which maps a (current state, input symbol) pair to a new state (see Figure 3 for an example). Given an input string $\sigma_1 \sigma_2 \dots$ and starting from the input state q_0 , at time $t \geq 1$ the FSM goes from state q_{t-1} to $q_t = \delta(q_{t-1}, \sigma_t)$.

The states $q_A, q_R \in Q$ are special terminal states, along with a special terminal character $\square \in \Sigma$ which only appears at the end of the input string. Every state $q \notin \{q_A, q_R\}$ satisfies $\delta(q, \square) \in \{q_A, q_R\}$. When the machine reaches state q_A or q_R , we say that it accepts or rejects the string, respectively.

Theorem 4 *Let $F = (Q, \Sigma, q_0, q_A, q_R, \delta)$ be an FSM. Consider a network consisting of an input area I and brain areas S and A , where I, S both have connections to and from area A , with interneurons D_S, D_A , where D_S disinhibits S upon input from A and D_A disinhibits A upon input from S . Suppose that for each $q \in Q, \sigma \in \Sigma$, there exist designated sets of k neurons $S_q \subseteq S, I_\sigma \subseteq I$, where $|S_q \cap S_r|, |I_\sigma \cap I_\rho| \leq \Delta = o(k)$ for all $q \neq r, \sigma \neq \rho$. Then if*

$$n \geq |Q|^2 |\Sigma|^2, \quad kp \geq 6 \ln n / k, \quad \beta \leq \frac{\ln \frac{n}{2kL}}{2(\max\{\Delta p, 6 \ln n\})^2}, \quad T \geq \frac{12}{\beta} \sqrt{\frac{\ln n}{kp}}$$

w.h.p. this network can simulate F on any input string $\sigma_1 \sigma_2 \dots \sigma_L$ in the following sense: If S_{q_0} is made to fire on round 1, and I_{σ_i} is made to fire on round $2i - 1$, $1 \leq i \leq L$, then after $2L + 2$ rounds, S_{q_A} will fire if F accepts the string and S_{q_R} will fire if F rejects the string.

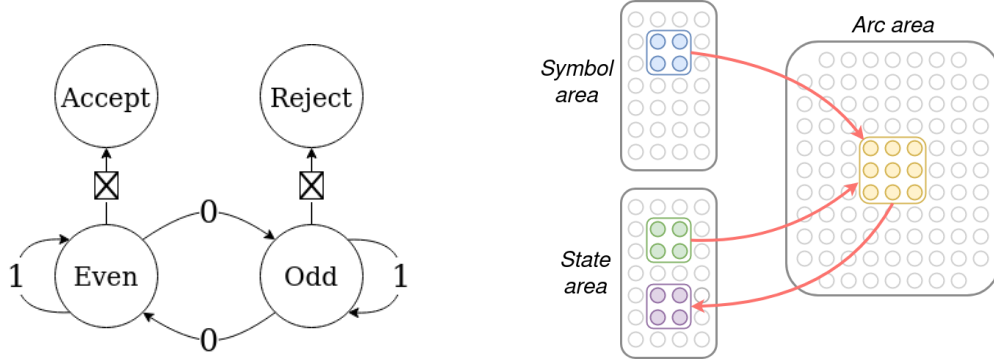


Figure 3: On the left is an example of a finite state machine (FSM), which consists of a finite number of states, joined by transitions (arrows). The machine changes states based on input symbols. This FSM accepts binary strings which contain an even number of zeros. On the right is the network architecture used here to simulate finite state machines. There is an assembly for each symbol, state, and transition; each pair of state and symbol assemblies projects to the associated arc assembly, which in turn projects back to the assembly corresponding to the state the FSM would switch to after seeing that state/symbol combination..

Note that by Lemma 3 if S fires on some round, A will be permitted to fire on the next, and vice versa. The crux of the simulation is to enable the configuration of synaptic weights of the network so that together, S_q and I_σ project to an assembly $A_{q,\sigma} \subseteq A$, and in turn $A_{q,\sigma}$ projects to $S_{\delta(q,\sigma)}$ (see Figure 3 for a schematic). As part of the proof, we will show that firing the sequence $\{S_q, I_\sigma\}, A_{q,\sigma}, S_{\delta(q,\sigma)}$ at least $7/\beta$ times will suffice to arrange this, so the FSM simulation can actually be configured by simply observing state transitions. With this in place, if S_q and I_σ fire together, two rounds later $S_{\delta(q,\sigma)}$ will fire, simulating a single transition of the FSM. So, with S_{q_0} firing initially and I_{σ_i} firing after $2L$ rounds, S_{q_A} (resp. S_{q_R}) will fire if the FSM accepts (resp. rejects). Hence, the behavior of the FSM on any input string $\sigma_1 \dots \sigma_L$ can be simulated in the projected FSM by setting S_{q_0} to fire initially in area S and presenting $I_{\sigma_1}, I_{\sigma_2}, \dots$ every other time step in area I . In Figure 9, we show assemblies simulating the FSM from Fig. 3.

An illustrative FSM. In Figure 4, we show assemblies simulating a FSM which recognizes strings which consist of the base 10 representation of a number divisible by 3. With 3 non-terminal states and an alphabet of 10 symbols, it operates by tracking the cumulative sum of the digits modulo 3, and accepts if this modulus is 0 at the end of the string (rejecting otherwise).

Remark 5 A finite-state transducer (a finite state machine that produces an output symbol with each transition) with output function $\theta: Q \times \Sigma \rightarrow \Gamma$ can be simulated using a third area B , which contains designated sets of k neurons B_γ for each $\gamma \in \Gamma$. To accomplish this, one simply fires $B_{\theta(q,\sigma)}$ at the same time as $S_{\delta(q,\sigma)}$ during training. Then, w.h.p., $B_{\theta(q,\sigma)}$ will fire two steps after A_q and I_σ under the same conditions on T .

2.4. Turing Completeness

A Turing Machine (TM) is an FSM together with a tape (read-write memory). Concretely, a single-tape TM is a tuple $M = (Q, \Sigma, \{L, R\}, q_0, q_A, q_R, \delta)$ where Q is a set of states, Σ is a set of tape

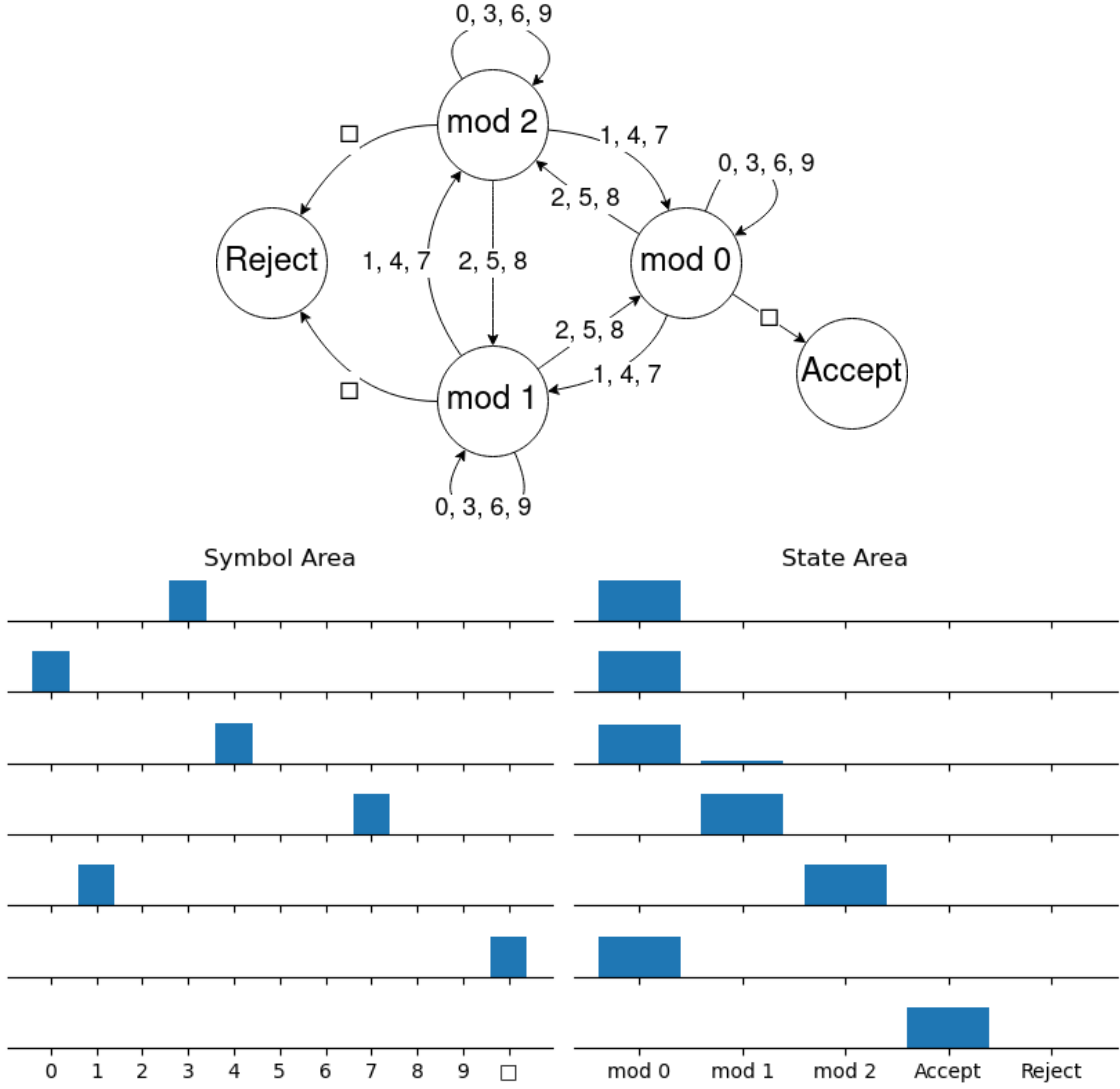


Figure 4: Above is the schematic of a FSM which accepts numbers in base 10 which are multiples of 3. The non-terminal states of the machine correspond to the remainder of the sum of digits which have been seen; the FSM accepts if the remainder at the end of the string is 0, and rejects otherwise. This FSM has a total of 5 states, 11 symbols, and 33 transitions. In the lower plot, we display the fraction of overlap between the responses of the trained model and the assemblies representing states and symbols, while simulating this FSM on the test string 30471. Here, $n = 5000$, $k = 70$, $p = 0.4$, $\beta = 0.1$, and the model was trained with 15 presentations of each transition.

symbols, q_0 is an initial state, and $\delta: Q \times \Sigma \rightarrow Q \times \Sigma \times \{L, R\}$ is a transition function. The TM has access to a tape of symbols, which initially has written on it the input to the machine, with an infinite number of blank space symbols (\sqcup) extending to the left and right of the input. The tape head of the TM indicates the current symbol, and begins at the first symbol of the input. The transition function of a Turing machine $\delta: Q \times \Sigma \rightarrow Q \times \Sigma \times \{L, R\}$ maps the current state and symbol indicated

by the tape head to a new state, a new symbol to write, and a direction to move the tape head. The operation of the machine is as follows: At each time step, when it is in state q , it reads a symbol σ from its tape. Denote the output of the transition function as $\delta(q, \sigma) = (r, \rho, d)$. It then (i) changes state to r , (ii) replaces σ with ρ on the current tape square, and (iii) moves to the square immediately left of the current one if $d = L$ and right if $d = R$. For simplicity in the simulation, we require that $\rho = \sigma$ if $d = L$, which is easily seen to maintain generality. Notably, the head of a Turing machine may be viewed as a finite state transducer which outputs symbols from the alphabet $\Sigma \times \{L, R\}$, writing symbols back to its (unbounded) input tape.

To simulate an arbitrary transition function, we augment the FSM network consisting of areas I, S, A with areas D and M , which are where movement commands and symbols to be written will be output (respectively). Areas I and M contain assemblies I_σ and M_σ , respectively, for each $\sigma \in \Sigma$, S contains an assembly S_q for each $q \in Q$, and D contains assemblies D_L and D_R . Now, as in Theorem 4, to implement a transition $\delta(q, \sigma) = (r, \rho, d)$, assemblies I_σ and S_q project to an assembly $A_{q,\sigma} \subseteq A$. In turn, $A_{q,\sigma}$ projects to S_r , M_ρ , and D_d .

What remains is to simulate the tape, namely maintain a sequence of symbols and a pointer location, and update both according to the output of the simulated transition function. We will show how to simulate a tape with assemblies, and thus (together with the FSM simulation) a Turing machine in its entirety, momentarily. The idea of the tape simulation is to maintain an assembly for each nonempty tape square, which projects to the assembly corresponding to the appropriate symbol. Each tape assembly is linked with those representing neighboring tape squares, and distributed across several brain areas configured so that when the FSM simulation issues a movement command, the assembly corresponding to the next tape square in the direction of movement will fire. To overwrite the current tape square, a new assembly is created and its connections with its neighbor and the new symbol are strengthened.

We remark that if the model instead has access to an external “tape”, we can achieve general computation with essentially just the FSM. For the environment to implement a tape, it suffices for it to contain a large number of distinguishable spaces, which can each store a representation of a symbol from Σ (imagine a stack of index cards and a writing implement). There is a pointer which indicates the current space, which is driven by the activity of the network such that it moves left or right when D_L or D_R fire in area D . If symbol σ is contained in the space indicated by the pointer, it causes I_σ to fire in area I ; and if M_σ fires, symbol σ is written to the space. The system consisting of the model and its environment will implement the action of the Turing machine with transition function δ on whatever is initially written on the external tape.

TAPE SIMULATION

To simulate the tape using assemblies, we split the tape into two halves and simulate each half independently. Each half-tape supports two operations: One operation adds a symbol to the beginning of the tape, while the other removes the current symbol so that the succeeding symbol is at the beginning. We implement this tape with assemblies as follows.

Intuitively, the tape is represented by a sequence of assemblies which cycle between the three areas, with the current position of the beginning of the tape represented by the currently firing assembly (see Figure 5). To remove the current symbol, the next area in the cycle is disinhibited, which causes the next assembly in the chain to fire (and the previous assembly is effectively forgotten); to add a new symbol, a new assembly is created in the preceding area, linked to the current assembly. The symbol at each position of the tape is stored by strengthened connections between

the tape assemblies and symbol assemblies in a designated symbol area, which will fire when the associated tape assemblies do. Precisely, the simulation consists of maintaining a set of assemblies $A_1(t), \dots, A_{L_t}(t)$ for $1 \leq t \leq T$ with the following properties:

- (i) If the t 'th operation adds σ to the beginning of the tape, with $A_1(t) \subseteq H_i$, we will have $A_1(t+1) \subseteq H_{i-1}$, and $A_{j+1}(t+1) = A_j(t-1)$ for all $1 \leq j \leq L_t$.
- (ii) If the t 'th operation removes σ from the beginning of the tape, we will have $A_i(t+1) = A_{i+1}(t)$ for all $1 \leq i \leq L_t - 1$.

A “delete” operation when assembly $A_1(t)$ in area H_i is firing will simply cause H_{i+1} to fire, and in turn strengthened connections from $A_1(t)$ to $A_2(t)$ will cause $A_2(t)$ to begin firing. An “add” operation is more complicated; with H_{i-1} disinhibited, input from outside of the tape areas will drive creation of a new assembly $A_1(t+1)$, which is linked to $A_1(t) = A_2(t+1)$ and S_σ (where σ is the symbol to be added to the tape) by their simultaneous firing. Thus, we require an lower bound on the plasticity, so that $A_1(t+1)$ can be formed quickly, as well as an upper bound on the plasticity, to ensure that existing assemblies in area H_{i-1} will not overlap $A_1(t+1)$ by too much. Three areas are required so that $A_1(t+1)$ becomes linked only in the forward direction to $A_1(t)$, and not in the backwards direction (i.e. in the future when $A_1(t+1)$ fires it will trigger $A_1(t) = A_2(t+1)$ to fire, but not vice versa).

Lemma 6 [Tape Simulation] *Consider three brain areas H_1, H_2, H_3 , each with n neurons, where H_i gives input to H_{i+1} (addition modulo 3) and all give input to an area S . The firing of H_i is governed by interneurons D_i , which receive input from a control area C containing assemblies C_{add} and C_{delete} . Suppose the behavior of D_i is as follows: D_i permits H_i to fire T times when either C_{add} fires together with H_i or H_{i+1} , OR C_{delete} and H_{i-1} fire together. Moreover, there are two areas E_1, E_2 , connected via interneurons which disinhibit E_1 for T rounds after E_2 fires T times, and disinhibit E_2 for T rounds after E_1 fires. Suppose that S initially contains assemblies S_σ for each $\sigma \in \Sigma$, with $|S_\sigma \cap S_\rho| \leq 6 \ln n$ for all $\sigma \neq \rho$. Let E be a set of neurons containing a set of k -caps Z_1, \dots, Z_L , where $|Z_t \cap Z_s| \leq 6 \ln n$ for all $t \neq s$, and Z_t fires on rounds $(t-1)T + 1$ through tT . Assume that*

$$\sqrt{\frac{\ln n}{kp}} \leq \beta \leq \frac{\ln \frac{n}{2kK}}{72 \ln^2 n}$$

and $kp \geq 3 \ln n$. Suppose there is a sequence of “add” and “delete” operations in the following sense: If the t th operation adds symbol σ , then C_{add} and S_σ are made to fire by external control on rounds $(t-1)T + 1$ through tT , while if the t th operation deletes the current symbol, then C_{delete} fires on rounds $(t-1)T + 1$ through tT . For a sequence of length $L \leq \frac{n}{2k}$, NEMO can simulate this sequence of operations: WHP, if σ is the current symbol on round t , then S_σ will fire on round $tT + 1$.

Now, by combining simulations of each tape half, we can simulate the entire tape. The symbol under the tape head is represented by the symbol at the beginning of the right half of the tape. A rightward movement of the TM is simulated by removing the first symbol from the right half of the tape, and adding the (potentially changed) symbol to the left half of the tape. A leftward movement is simulated by removing the first symbol from the left half and adding it to the right half (recall that the symbol does not change in a leftward movement). As a consequence, NEMO is Turing complete.

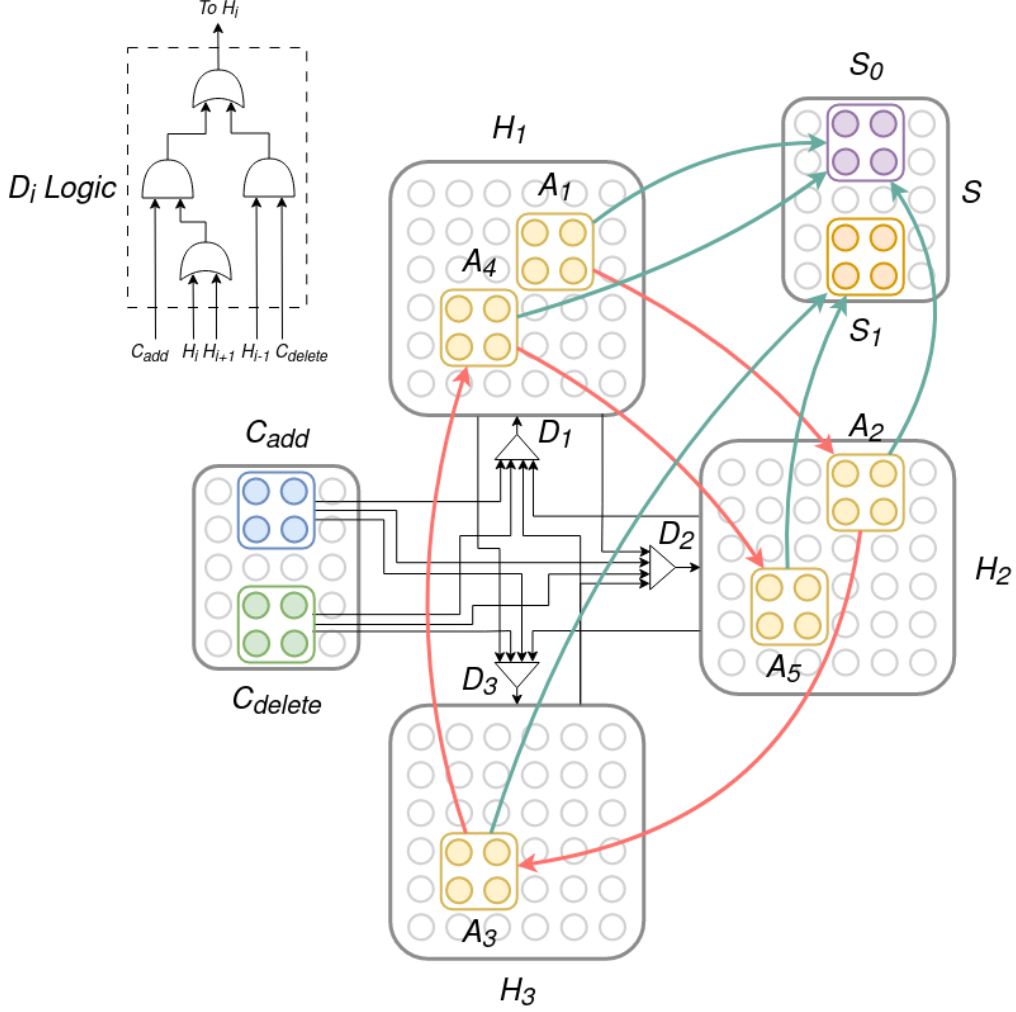


Figure 5: Simulating a restricted tape with assemblies. Assemblies A_1, \dots, A_5 each represent a space on the tape, and are placed to cycle between areas H_1, H_2, H_3 (red arrows). C_{add} and C_{delete} are externally-activated control assemblies, which signal operations to areas H_1, H_2, H_3 and via interneuron populations D_1, D_2, D_3 determine the sequence in which they are disinhibited. On the upper left we provide a schematic of the logical function implemented by D_i , which carries out the inhibition and disinhibition of H_i to simulate the operations signalled by the control assemblies. Black arrows in the larger diagram correspond to inputs to (i.e. synapses of) the interneurons, D_1, D_2, D_3 . To represent symbol σ being written at space i , assembly A_i is linked to assembly S_σ (teal connections) so that the firing of A_i will cause S_σ to fire. At this point in the simulation, the simulated tape has the string 00101 written on it.

The simulation consists of six areas $H_i^L, H_i^R, i = 1, 2, 3$, three each for the “left” and “right” halves of the tape, a control area D for both halves jointly, and the three areas I, S, A for the FSM, which yields a total of 10 areas ($2 \times 3 + 1 + 3$). The outline of its operation is as follows: The FSM simulation proceeds as in Theorem 4, modified so that if $\delta(q, \sigma) = (p, \rho, d)$, the assembly $A_{q, \sigma}$ causes S_p, I_ρ , and D_d to fire, where $d \in \{L, R\}$. The tape halves are simulated as in Lemma 6, where the firing of D_L signals a “delete” operation for the left tape and an “add” operation for the right tape (and vice versa). The new assembly on the right half becomes linked to I_ρ by their concurrent firing, which effects a leftward movement of the tape head (and similarly for D_R).

Theorem 7 [TM Simulation] *With plasticity*

$$\sqrt{\frac{\ln n}{kp}} \leq \beta \leq \frac{\ln \frac{n}{2kT}}{72 \log^2 n}$$

and $kp \geq 3 \ln n$, w.h.p. NEMO can simulate a Turing machine $M = (Q, \Sigma, \{L, R\}, q_0, q_A, q_R, \delta)$ which uses T time in time $O(T)$ using ten brain areas, each of size $n \geq 2 \max\{T^2, |Q|^2 |\Sigma|^2\}$.

3. Experiments

To support our theoretical results, we have simulated the sequence and FSM models extensively. We detail the results and conclusions of these various experiments here.

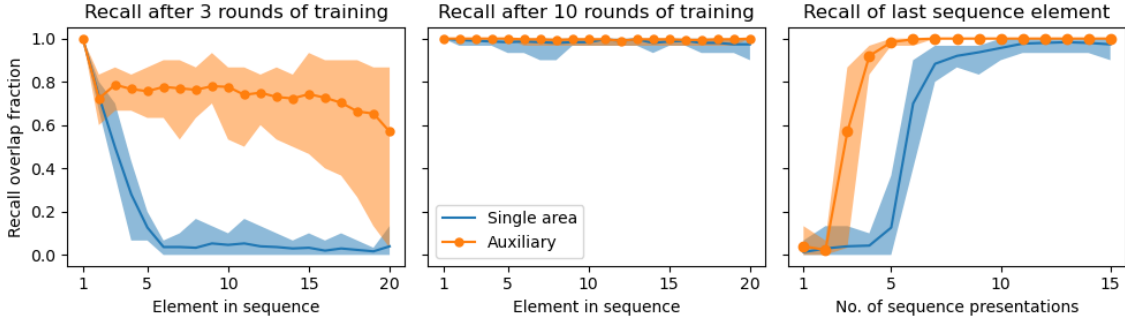


Figure 6: Simple vs scaffold sequence memorization: we examine recall of the sequence in response to presentation of only the first item after 3 (left) and 10 (center) presentations of the sequence, by measuring the fraction of neurons in the assembly corresponding to a given element of the sequence which fire during testing. On the right, we demonstrate how the recall of the last element of the sequence (again, after only the first is presented) over the course of training. Here, $n = 1000$, $k = 30$, $p = 0.2$, $\beta = 0.1$, and the sequence is length 20. Dark center line is the mean over 10 trials, while shaded area is the range.

Number of presentations versus recall. In Figure 6 we show how recall of a sequence improves over the course of repeated presentations, for both the single-area and scaffolded models. Significantly, the faster rate of memorization observed for the scaffolded model supports the bound given in Theorem 2. Here, we estimate the assembly corresponding to a given element in the sequence as the set of neurons which fire on the last round of training, and measure recall as the fraction

of neurons in that assembly which fire at the appropriate time when only the first element of the sequence is presented.

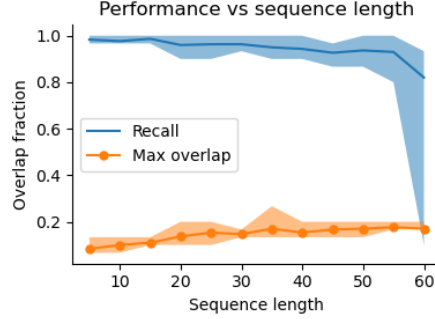


Figure 7: For each choice of sequence length, we train the model via repeated presentations of a sequence of the given length. In blue we plot the recall of the last element in the sequence, and in orange we plot the maximum overlap of assemblies corresponding to distinct sequence elements. Here, $n = 1000$, $k = 30$, $p = 0.2$, $\beta = 0.1$, and each sequence is trained via 10 presentations. Dark center line is the mean over 10 trials, while shaded area is the range.

Sequence memorization capacity. In Figure 7, we increase the length of the sequence to be memorized and measure both the recall of the sequence and the maximum overlap between assemblies corresponding to different sequence elements. This disambiguates two failure modes of sequence learning, where either different neurons fire during testing versus training or the assemblies representing different sequence elements become indistinguishable. Notably, the capacity of a given brain area seems to greatly exceed the bound we give in Theorem 1, and indeed even surpasses the quantity n/k which is the largest number of disjoint k -caps which can be formed in a given area. This suggests that sequence learning in NEMO is significantly more robust than our analysis implies.

Effect of parameters on sequence memorization. We examine the effect of area size (Figure 8, left) and edge density (Figure 8, right) on the success of sequence memorization. In each case, we vary the relevant parameter while training the model to memorize a length 25 sequence, and measure the fraction of neurons in the last assembly of the sequence which fire at the appropriate time when only the first element of the sequence is presented (*recall*), and the largest fraction of overlap between any two assemblies corresponding to distinct elements (*max overlap*). High recall indicates that the neural responses to the sequence of stimuli have been memorized, while low max overlap indicates that the assemblies corresponding to any pair of distinct sequence elements are distinguishable. Our analytical results (where the probability of success increases with n , and we require the product kp to be sufficiently large) predict that increasing either parameters should improve performance (i.e. increase recall and decrease overlap) which is indeed observed experimentally. Notably, reasonably good performance is attained for substantially larger ranges of n and p than we require in the theorems.

FSM memorization. In Figure 9 we demonstrate how the performance of each transition of the FSM improves over the course of training, and how performance degrades as the size of the FSM (i.e. total number of transitions) increases, while all parameters of the model are fixed. We measure

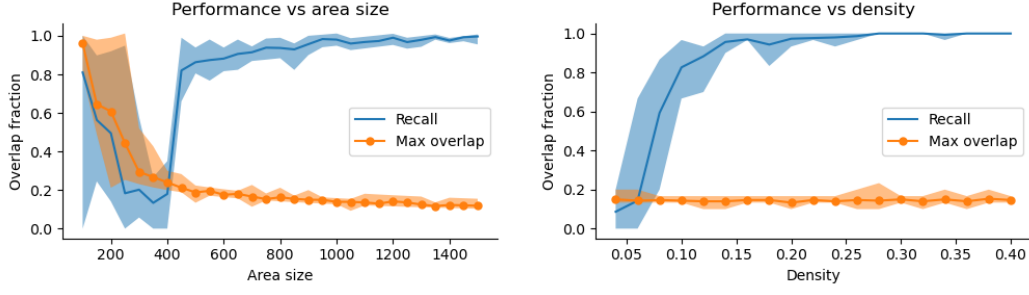


Figure 8: We measure performance of sequence memorization as two key parameters of the model (area size and density of connections) are varied. On the left, we vary n from 100 to 1500 while $k = \sqrt{n}$, $p = 0.2$, $\beta = 0.1$. On the right, we vary p from 0.04 to 0.4 while $n = 1000$, $k = 30$, $\beta = 0.1$. In both cases the sequence to be memorized is length 25 and training consists of 10 presentations. Dark center line is the average over 10 trials, while shaded area is the range.

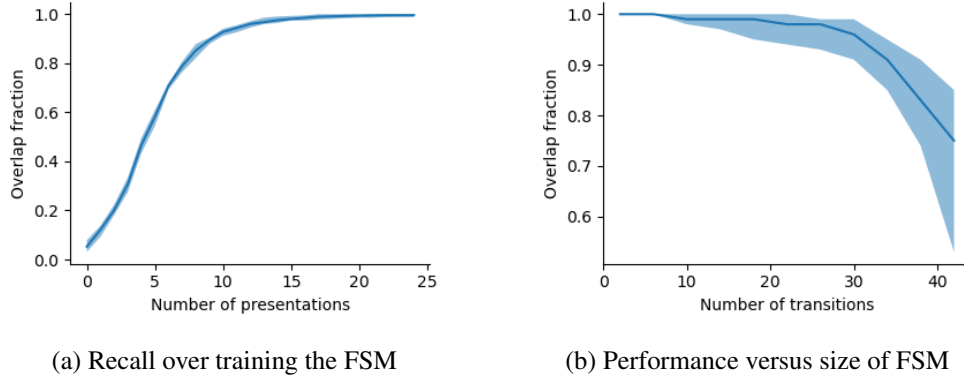


Figure 9: In (a), we train the model by repeatedly presenting each transition of the FSM in Figure 3 and measure performance after a given number of presentations. In (b), we train the model using FSMs of different sizes and again measure the recall. Here, $n = 5000$, $k = 70$, $p = 0.4$, $\beta = 0.1$ and the model is trained with 15 presentations of each transition. Dark center line indicates mean over 10 trials; shaded area indicates the range.

performance by the recall averaged over all transitions, where here the recall is the fraction of neurons in the appropriate next state assembly which fire two rounds after the assemblies corresponding to a given state/symbol pair are made to fire.

Effect of parameters on FSM memorization. We examine the effect of area size (Figure 10, left) and edge density (Figure 10, right) on the success of FSM memorization. Using the FSM simulated in Figure 4 (see Figure 4 for a diagram), we vary the relevant parameter while training the model to memorize each transition of this FSM. We measure performance through the fraction of neurons in the appropriate next state assembly which fire two rounds after the assemblies corresponding to a given state/symbol pair are made to fire (*recall*), with the minimum taken over all transitions, and the fraction of a random sample of length 20 input strings which are correctly accepted or rejected (*classification accuracy*), in the sense that the state assembly with the most neurons firing on the last

round corresponds to the correct terminal state. Our analytical results (where again the probability of success increases with n , and we require the product kp to be sufficiently large) predict that increasing either n or p should improve performance (i.e. increase both recall and classification accuracy) which is observed experimentally. Notably, classification accuracy reaches a perfect score much sooner than recall.

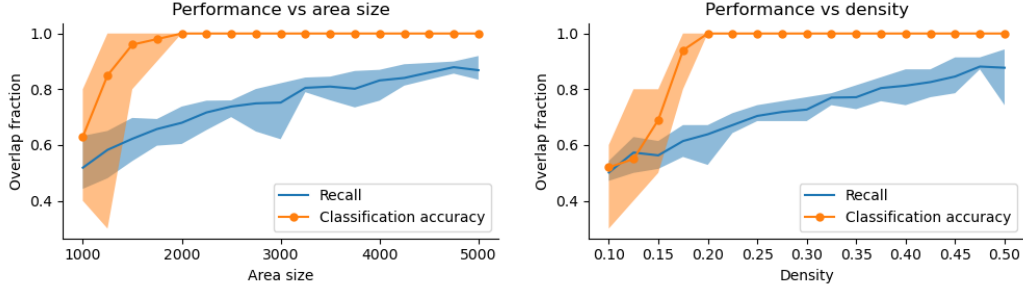


Figure 10: We measure performance of FSM memorization as two key parameters of the model (area size and density of connections) are varied. On the left, we vary n from 1000 to 5000 while $k = \sqrt{n}$, $p = 0.5$, $\beta = 0.1$. On the right, we vary p from 0.1 to 0.5 while $n = 5000$, $k = 70$, $\beta = 0.1$. In both cases the FSM is given in Figure 4 (with 11 symbols and 3 non-terminal states) and training consists of 15 presentations of each transition. Dark center line is the average over 10 trials, while shaded area is the range.

Effect of input string length on FSM simulation. We examine the effect of the length of the input string on the accuracy of the simulation of the FSM on it (Figure 11). For a few choices of the key parameters (area size n and density p), we train the model to memorize each transition of the FSM in Figure 4 and then test its performance on a random sample of input strings of various sizes. As above, we measure performance via *classification accuracy*, the fraction of strings which are correctly accepted or rejected (i.e. the state assembly with the most neurons firing on the last round corresponds to the correct terminal state). For n and p such that all transitions are performed accurately, we expect that classification accuracy should be very high even for long strings, while for smaller n and p classification accuracy should decay with string length. This is largely supported by the simulations, where classification accuracy remains nearly perfect for all string lengths for the larger choices of n and p and decays somewhat for the smaller choices, although notably even for long strings the classification accuracy is still substantially higher than chance (which would be 0.2 with the 5 states of the FSM).

4. Proofs

Proof sketches. All of our proofs rely on a few basic ingredients. A key observation underpinning all of them is that in the range of parameters assumed, the neurons which activate in response to a given sequence element/transition do not change over the course of training w.h.p. Intuitively, if the weights change sufficiently slowly, then repeated presentations of the same stimulus should activate the same set of neurons. We then show that the overlap of assemblies corresponding to distinct sequence elements/transitions will not be too large, which will allow them to be distinguished and ensures that increasing weights between one pair of assemblies will not interfere with others.

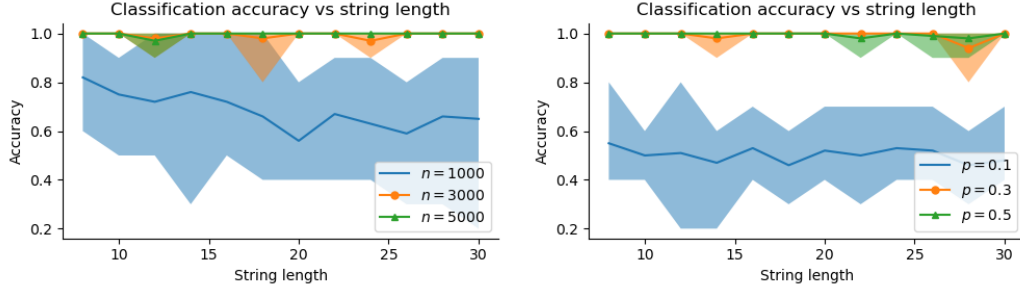


Figure 11: We measure performance of FSM simulation as the length of the input string increases, for a few choices of area size (left) and edge density (right). On the left, $k = \sqrt{n}$, $p = 0.5$, $\beta = 0.1$; on the right, $n = 5000$, $k = 70$, $\beta = 0.1$. In both cases the FSM is given in Figure 4 (with 11 symbols and 3 non-terminal states) and training consists of 15 presentations of each transition. Dark center line is the average over 10 trials, while shaded area is the range.

Finally, we bound the number of rounds of training needed to ensure that recall occurs successfully, which simply involves comparing the input a neuron in the correct assembly will receive versus a neuron outside of the correct assembly, and choosing the weight to be sufficiently high so that the neurons in the correct assembly have the highest input w.h.p.

To proceed with the proofs in full, we first need a few crucial lemmas. Given a pair of inputs to a brain area, Lemma 8 provides an upper bound (which depends on the overlap of these inputs) on the overlap of the sets of neurons which fire in response to them, when plasticity is in effect.

Lemma 8 *Let $\delta > 0$. Let I_1, I_2 be sets of neurons providing input to brain area A . (Note that I_1, I_2 might intersect A .) Suppose that I_1 fires, forming a cap C_1 , with weights from I_1 to C_1 increased by $1 + \gamma$. Some time later I_2 fires, forming a cap C_2 . Suppose that $|I_1|, |I_2| \geq k$, and that $kp \geq 6 \ln \frac{n}{k}$. Then if $|I_1 \cap I_2| = 0$, we have*

$$\Pr \left[|C_1 \cap C_2| \geq 2 \max \left\{ \frac{k^2}{n}, 3 \ln \frac{1}{\delta} \right\} \right] \leq \delta$$

and otherwise, for $\epsilon \geq k/n$ and

$$\gamma \leq \frac{\sqrt{3|I_2|p \ln \frac{n}{k}} - \max \left\{ \sqrt{3|I_1 \cap I_2|p \ln \frac{2n}{\delta}}, 3 \ln \frac{2n}{\delta} \right\} - \sqrt{3|I_2 \setminus I_1|p \ln \frac{2}{\epsilon}}}{2 \max \left\{ |I_1 \cap I_2|p, 3 \ln \frac{2n}{\delta} \right\}}$$

we have

$$\Pr \left[|C_1 \cap C_2| \geq \max \left\{ \epsilon k, 6 \ln \frac{2}{\delta} \right\} \right] \leq \delta$$

Lemma 9 controls the number of caps a given neuron will enter in response to a sequence of stimuli with bounded overlap.

Lemma 9 *Let I_1, \dots, I_L be a set of inputs to a brain area A (which might intersect A) which are presented in sequence, satisfying $|I_1| \geq k$, $|I_t| = m \geq k$ for all $t > 1$, $|I_s \cap I_t| \leq \Delta$ for all $s \neq t$, and*

$$L \leq 3 \ln n \left(\frac{n}{k} \right)^{(1 - \sqrt{\frac{\Delta \ln n}{m \ln \frac{n}{k}}})^2}$$

Let C_t denote the cap denoting from I_t , and $\mathbb{1}_t$ denote the indicator vector for C_t . Then for

$$\beta \leq \frac{(1 - \sqrt{\frac{\Delta \ln n}{m \ln \frac{n}{k}}})^2 \ln \frac{n}{k} - \ln L - \frac{1}{3}}{2(\max\{\Delta p, 6 \ln n\})^2}$$

and $kp \geq 3 \ln n$ we have

$$\sum_{t=1}^L \mathbb{1}_t(i) < 6 \ln n$$

w.h.p. for all $i \in A$.

Lemma 10 provides a criterion to ensure that the same set of neurons will fire in response to the same stimulus.

Lemma 10 *Let $\delta > 0$, and let I be a set of neurons providing input to brain area A with $|I|p \geq 3 \ln \frac{1}{\delta}$. Let $C \subseteq A$ be a set of k neurons, where each neuron in C has at least d incoming edges from I , each strengthened by a factor of $1 + \gamma$. Suppose no neuron outside of C has more than m incoming connections from C which have been strengthened, each by a factor no more than $1 + c\gamma$. Then for*

$$\gamma \geq \frac{|I|p + \sqrt{3|I|p \ln \frac{n}{\delta}} - d}{d - cm}$$

if I fires, the resulting cap C' will equal C w.p. $1 - \delta$

Lemma 11 upper bounds the overlap of the caps for a pair of stimuli, at a larger overlap than Lemma 8.

Lemma 11 *Let I_1 and I_2 be two sets of neurons providing input to area A , with $|I_1| = |I_2| = 2k$ and $|I_1 \cap I_2| \leq (1 + o(1))k$, and let A_1, A_2 denote their respective caps. Then*

$$|A_1 \cap A_2| \leq \frac{k}{2}$$

w.p. $1 - o(n^{-1})$.

Finally, Lemma 12 is a fact about the fixed points of a certain class of exponential functions.

Lemma 12 *Let $f(x) = \exp(-a(b(1 - x)^2 - 1))$ for $a > 0, b \geq 1 + 2a^{-1}$. Then there exists some $x^* \in \mathbb{R}$ such that $f(x^*) = x^*$ and moreover*

$$x^* \leq \exp(-a(b - 1))$$

We can now proceed with the proofs of the theorems.

Proof [Proof of Theorem 1] We will first show that on the first presentation, the overlap between the sets of neurons which fire for different elements of the sequence will not be too large for sufficiently small plasticity. Using this fact, we can then show that the sequence of neurons which fire will remain the same over repeated presentations of the stimulus sequence. Finally, this second claim makes it simple to show that after enough presentations the sequence of neurons will be strongly

linked enough that when only the first cap fires, the rest of the sequence will as well without external stimulus.

We will prove the first claim by induction on σ . The base case $\sigma = 1$ holds vacuously. For $\sigma \geq 1$, we note that if $|A_\rho(1) \cap A_\sigma(1)| \leq 6 \ln \frac{n}{k}$ for all $\rho < \sigma$, then the input to $A_{\sigma+1}(1)$ ($S_{\sigma+1}$ and $A_\sigma(1)$) overlaps the input to any other set $A_\rho(1)$ by at most $\Delta + 6 \ln \frac{n}{k}$. As weights are increased by $1 + \beta$ and

$$\beta \leq \frac{\ln \frac{n}{kL} - \frac{1}{3}}{2(\max\{\Delta p, 6 \ln n\})^2} \leq \frac{\sqrt{6kp \ln \frac{n}{k}} - \max\{\sqrt{6\Delta p \ln Ln}, 6 \ln nL\} - \sqrt{6kp \ln k}}{2 \max\{\Delta p, 6 \ln \frac{n}{k}\}}$$

by Lemma 8 we have $|A_{\sigma+1}(1) \cap A_\rho(1)| \leq 6 \ln \frac{n}{k}$ w.p. $1 - o(L^{-2})$ as well. A union bound over all $O(L^2)$ events shows that the probability that $|A_\sigma(1) \cap A_\rho(1)| > 6 \ln \frac{n}{k}$ for any pair $\rho \neq \sigma$ is $o(1)$.

We will now show that $A_\sigma(t) = A_\sigma(1)$ for all σ , by first proving that $A_\sigma(2) = A_\sigma(1)$ via induction on σ . First note that, by Lemma 9, no neuron in A makes more than $6 \ln n$ caps $A_1(1), \dots, A_L(1)$ w.h.p. Let $X_i(t, \sigma)$ denote the input to i on round t during presentation of S_σ . For the base case $\sigma = 1$, for $i \in A_1(1)$, we have

$$e(S_1, i) \geq kp + \sqrt{3kp \ln \frac{n}{k}}$$

and so its input is

$$X_i(2, 1) \geq \frac{(1 + \beta)(kp + \sqrt{3kp \ln \frac{n}{k}})}{2np + 2\beta kp}$$

while for $j \notin A_1(1)$,

$$\begin{aligned} X_j(2, 1) &\leq \frac{kp + \sqrt{3kp \ln \frac{n}{k}} + (1 + \beta)^{6 \ln n}(\Delta p + \max\{\Delta p, 3 \ln n\})}{2np + (1 + \beta)^{6 \ln n}(\Delta p + \max\{\Delta p, 3 \ln n\})} \\ &\leq \frac{kp + \sqrt{3kp \ln \frac{n}{k}} + 2(1 + \beta)^{6 \ln n} \max\{\Delta p, 3 \ln n\}}{2np + (1 + \beta)^{6 \ln n}(\Delta p + \max\{\Delta p, 3 \ln n\})} \end{aligned}$$

Observe that for

$$\beta \leq \frac{\ln \frac{n}{kL} - \frac{1}{3}}{2(\max\{\Delta p, 6 \ln n\})^2} \leq \frac{1}{6 \ln n}$$

we have

$$X_j(2, 1) \leq \frac{(1 + \beta)(kp + \sqrt{3kp \ln \frac{n}{k}})}{2np + 2\beta kp}$$

in which case $X_i(2, 1) > X_j(2, 1)$ for all $i \in A_1(1), j \notin A_1(1)$.

Now assume that $\sigma > 1$ and $A_\rho(2) = A_\rho(1)$ for all $\rho < \sigma$. For $i \in A_\sigma(1)$,

$$e(S_\sigma \cup A_{\sigma-1}(1), i) \geq 2kp + \sqrt{6kp \ln \frac{n}{k}}$$

and so

$$X_i(2, \sigma) \geq \frac{(1 + \beta)(2kp + \sqrt{6kp \ln \frac{n}{k}})}{np + \beta 2kp + \sqrt{6kp \ln \frac{n}{k}}}$$

On the other hand, for all $j \notin A_\sigma(1)$, we have

$$X_j(2, \sigma) \leq \frac{2kp + \sqrt{6kp \ln \frac{n}{k}} + 4(1 + \beta)^{6 \ln n} \max\{\Delta p, 3 \ln n\}}{np + 4(1 + \beta)^{6 \ln n} \max\{\Delta p, 3 \ln n\}}$$

For

$$\beta \leq \frac{\ln \frac{n}{kL} - \frac{1}{3}}{2(\max\{\Delta p, 6 \ln n\})^2} \leq \frac{1}{12 \ln n}$$

we have

$$X_j(2, \sigma) \leq \frac{(1 + \beta)(2kp + \sqrt{6kp \ln \frac{n}{k}})}{np + \beta 2kp + \sqrt{6kp \ln \frac{n}{k}}}$$

and so $X_i(2, \sigma) > X_j(2, \sigma)$ for all $i \in A_\sigma(1), j \notin A_\sigma(1)$, which means $A_\sigma(2) = A_\sigma(1)$.

Now, we use double induction on t and σ , with $t = 2$ as the base case. Let $X_i(\sigma, t)$ denote the input to neuron i when S_σ fires on round t . Suppose that $A_\rho(s) = A_\rho(1)$ for all ρ and $s < t$ and $A_\rho(t) = A_\rho(1)$ for all $\rho < \sigma$. For $i \in A_\sigma(1)$, we have

$$X_i(t, \sigma) \geq \frac{(1 + \beta)X_i(t-1, \sigma)}{2np + \beta X_i(t-1, \sigma)}$$

For $j \notin A_\sigma(1)$,

$$X_j(t, \sigma) \leq \frac{X_j(t-1, \sigma) + (e^{6\beta \ln n} - 1)(X_j(t-1, \sigma) - 2kp - \sqrt{6kp \ln \frac{n}{k}})}{2np + (e^{6\beta \ln n} - 1)(X_j(t-1, \sigma) - 2kp - \sqrt{6kp \ln \frac{n}{k}})}$$

For

$$\beta \leq \frac{\ln \frac{n}{kL} - \frac{1}{3}}{2(\max\{\Delta p, 6 \ln n\})^2} \leq \frac{(1 - \sqrt{\frac{\Delta \ln n}{k \ln \frac{n}{k}}})^2 \ln \frac{n}{k} - \ln L - \frac{1}{3}}{2(\max\{\Delta p, 6 \ln n\})^2}$$

and $\Delta \leq k / \ln^2 n$, we have $X_j(t, \sigma) \leq X_i(t, \sigma)$ and hence, $A_\sigma(t) = A_\sigma(1)$.

Now, we will prove the last claim. For $\sigma = 1$, the argument is the same as during training since S_1 still fires, so we have $\hat{A}_\sigma = A_\sigma(1)$. Suppose that $|\hat{A}_{\sigma-1} \cap A_{\sigma-1}(1)| = (1 - \epsilon)k$. Then for $i \in A_\sigma(1)$,

$$X_i(\sigma) \geq \frac{(1 - \epsilon)(1 + \beta)^T(kp + \sqrt{\frac{3}{2}kp \ln \frac{n}{k}}) + \epsilon kp}{((1 + \beta)^T - 1)(kp + \sqrt{3kp \ln \frac{n}{k}}) + 2np} = \tau_\epsilon$$

while for $j \notin A_\sigma(1)$,

$$X_j(\sigma) \sim \frac{\mathcal{B}(k, p)}{2np}$$

Hence,

$$\begin{aligned} \Pr[j \in \hat{A}_\sigma \mid j \notin A_\sigma(1)] &\leq \Pr[X_j(\sigma) \geq \tau_\epsilon] \\ &\leq \exp \left(-\frac{1}{3kp} \left((1 - \epsilon)\beta T(kp + \sqrt{\frac{3}{2}kp \ln \frac{n}{k}}) + (1 - \epsilon)\sqrt{\frac{3}{2}kp \ln \frac{n}{k}} \right)^2 \right) \\ &\leq \exp \left(-\frac{1}{2}(1 - 2\epsilon)(1 + 2\beta T)^2 \ln \frac{n}{k} \right) \end{aligned}$$

The fraction of newcomers is hence, in expectation, no more than

$$\frac{n}{k} \exp \left(-\frac{1}{2}(1-2\epsilon)(1+2\beta T)^2 \ln \frac{n}{k} \right)$$

We seek a fixed point ϵ^* of this function. By Lemma 12, we have

$$\epsilon^* \leq \left(\frac{k}{n} \right)^{2\beta T}$$

as long as

$$T \geq \frac{1}{\beta \ln \frac{n}{k}}$$

Now, for perfect recall, suppose that

$$T \geq \frac{1}{\beta} \sqrt{\frac{\ln n L}{2 \ln \frac{n}{k}}}$$

Then

$$\exp \left(-\frac{1}{2}(1+2\beta T)^2 \ln \frac{n}{k} \right) \leq \frac{1}{nL}$$

Then a union bound over vertices and $1 \leq \sigma \leq L$ shows that the probability $\hat{A}_\sigma \neq A_\sigma(1)$ for some σ is $o(1)$. \blacksquare

Proof [Proof of Theorem 2] The argument proceeds similarly as in the proof of Theorem 1: We bound the overlap of different caps during the first presentation, show that the sequence of caps will remain the same over subsequent presentations, and show that after enough presentations the sequence of caps will be recalled without external input after the first round. Crucially, a larger fraction of the input to the correct neurons in the main area will still fire in the absence of external stimuli, which allows memorization to occur more quickly than in the absence of the auxiliary area.

We will prove the first claim by induction on σ . The base case $\sigma = 1$ holds vacuously. For $\sigma \geq 1$, we note that if $|A_\rho(1) \cap A_\sigma(1)| \leq 6 \ln \frac{n}{k}$ for all $\rho < \sigma$, and $|B_\rho(1) \cap B_\sigma(1)| \leq 6 \ln \frac{n}{k}$ for all $\rho < \sigma - 1$, then the input to $A_{\sigma+1}(1)$ ($S_{\sigma+1}$, $A_\sigma(1)$, and $B_{\sigma-1}(1)$) overlaps the input to any other set $A_\rho(1)$ by at most $\Delta + 12 \ln \frac{n}{k}$. As weights are increased by $1 + \beta$ and

$$\beta \leq \frac{\ln \frac{n}{kL} - \frac{1}{3}}{2(\max\{\Delta p, 6 \ln n\})^2} \leq \frac{\sqrt{9kp \ln \frac{n}{k}} - \max\{\sqrt{9\Delta p \ln Ln}, 3 \ln nL\} - \sqrt{9kp \ln k}}{3 \max\{\Delta p, 6 \ln \frac{n}{k}\}}$$

by Lemma 8 we have $|A_{\sigma+1}(1) \cap A_\rho(1)| \leq 6 \ln \frac{n}{k}$ w.p. $1 - o(L^{-2})$ as well. The argument proceeds similarly for $B_\sigma(1)$. Then a union bound over all $O(L^2)$ events shows that the probability that $|A_\rho(1) \cap A_\sigma(1)|$ or $|B_\rho(1) \cap B_\sigma(1)| > 6 \ln \frac{n}{k}$ for any pair $\sigma \neq \rho$ is $o(1)$.

We will now show that $A_\sigma(t) = A_\sigma(1)$ and $B_\sigma(t) = B_\sigma(1)$ for all σ . We note that, by Theorem 1, $B_\sigma(t) = B_\sigma(1)$ for all σ and t w.h.p. as long as $A_\rho(s) = A_\rho(1)$ for all pairs (ρ, s) where either $s < t$ or $\rho < \sigma$. So, it will suffice to only show that $A_\sigma(s) = A_\sigma(1)$, which we will accomplish by first proving that $A_\sigma(2) = A_\sigma(1)$ via induction on σ . First note that, by Lemma 9, no neuron in A makes more than $6 \ln n$ caps $A_1(1), \dots, A_L(1)$. Let $X_i(t, \sigma)$ denote the input to i on round t during presentation of S_σ . For the base case $\sigma = 1$, for $i \in A_1(1)$, we have

$$e(S_1, i) \geq kp + \sqrt{3kp \ln \frac{n}{k}}$$

and so its input is

$$X_i(2, 1) \geq \frac{(1 + \beta)(kp + \sqrt{3kp \ln \frac{n}{k}})}{2np + 2\beta kp}$$

while for $j \in A \setminus A_1(1)$,

$$\begin{aligned} X_j(2, 1) &\leq \frac{kp + \sqrt{3kp \ln \frac{n}{k}} + (1 + \beta)^{6 \ln n} (\Delta p + \max\{\Delta p, 3 \ln n\})}{2np + (1 + \beta)^{6 \ln n} (\Delta p + \max\{\Delta p, 3 \ln n\})} \\ &\leq \frac{kp + \sqrt{3kp \ln \frac{n}{k}} + 2(1 + \beta)^{6 \ln n} \max\{\Delta p, 3 \ln n\}}{2np + (1 + \beta)^{6 \ln n} (\Delta p + \max\{\Delta p, 3 \ln n\})} \end{aligned}$$

Observe that for

$$\beta \leq \frac{\ln \frac{n}{kL} - \frac{1}{3}}{2(\max\{\Delta p, 6 \ln n\})^2} \leq \frac{1}{6 \ln n}$$

we have

$$X_j(2, 1) \leq \frac{(1 + \beta)(kp + \sqrt{3kp \ln \frac{n}{k}})}{2np + 2\beta kp}$$

in which case $X_i(2, 1) > X_j(2, 1)$ for all $i \in A_1(1), j \in A \setminus A_1(1)$. Hence, $A_2(1) = A_1(1)$.

Now let $\sigma > 1$, and assume that $A_\rho(2) = A_\rho(1)$ and $B_{\rho-1}(2) = B_{\rho-1}(1)$ for all $\rho < \sigma$. For $i \in B_{\sigma-1}(1)$,

$$e(A_{\sigma-1} \cup B_{\sigma-2}(1), i) \geq 2kp + \sqrt{6kp \ln \frac{n}{k}}$$

and so

$$X_i(2, \sigma) \geq \frac{(1 + \beta)(2kp + \sqrt{6kp \ln \frac{n}{k}})}{2np + \beta 2kp + \sqrt{6kp \ln \frac{n}{k}}}$$

On the other hand, for all $j \in B \setminus B_{\sigma-1}(1)$, we have

$$X_j(2, \sigma) \leq \frac{2kp + \sqrt{6kp \ln \frac{n}{k}} + 12(1 + \beta)^{6 \ln n} \ln \frac{n}{k}}{2np + 12(1 + \beta)^{6 \ln n} \ln n}$$

For

$$\beta \leq \frac{\ln \frac{n}{kL} - \frac{1}{3}}{2(\max\{\Delta p, 6 \ln n\})^2} \leq \frac{1}{12 \ln n}$$

, we have

$$X_j(2, \sigma - 1) \leq \frac{(1 + \beta)(2kp + \sqrt{6kp \ln \frac{n}{k}})}{2np + \beta 2kp + \sqrt{6kp \ln \frac{n}{k}}}$$

and so $X_i(2, \sigma) > X_j(2, \sigma)$ for all $i \in B_{\sigma-1}(1), j \in B \setminus B_{\sigma-1}(1)$, which means $B_{\sigma-1}(2) = B_{\sigma-1}(1)$. Then, for $i \in A_\sigma(1)$,

$$e(S_\sigma \cup A_\sigma(1) \cup B_{\sigma-1}(1), i) \geq 3kp + \sqrt{9kp \ln \frac{n}{k}}$$

and so

$$X_i(2, \sigma) \geq \frac{(1 + \beta)(3kp + \sqrt{9kp \ln \frac{n}{k}})}{3np + \beta 3kp + \sqrt{9kp \ln \frac{n}{k}}}$$

On the other hand, for all $j \in A \setminus A_\sigma(1)$, we have

$$X_j(2, \sigma) \leq \frac{3kp + \sqrt{6kp \ln \frac{n}{k}} + 12(1 + \beta)^{6 \ln n} \ln \frac{n}{k}}{3np + 12(1 + \beta)^{6 \ln n} \ln n}$$

For

$$\beta \leq \frac{\ln \frac{n}{kL} - \frac{1}{3}}{2(\max\{\Delta p, 6 \ln n\})^2} \leq \frac{1}{12 \ln n}$$

we have

$$X_j(2, \sigma) \leq \frac{(1 + \beta)(3kp + \sqrt{9kp \ln \frac{n}{k}})}{3np + \beta 3kp + \sqrt{9kp \ln \frac{n}{k}}}$$

and so $X_i(2, \sigma) > X_j(2, \sigma)$ for all $i \in A_\sigma(1), j \in A \setminus A_\sigma(1)$, so $A_\sigma(2) = A_\sigma(1)$. Then using induction, we have $A_\sigma(2) = A_\sigma(1)$ and $B_\sigma(2) = B_\sigma(1)$ for all $1 \leq \sigma \leq L$.

Now, we use double induction on t and σ , with $t = 2$ as the base case. Let $X_i(t, \sigma)$ denote the input to neuron i when S_σ fires on round t . Suppose that $A_\rho(s) = A_\rho(1)$ and $B_{\rho-1}(s) = B_{\rho-1}(1)$ for all ρ and $s < t$ and $A_\rho(t) = A_\rho(1)$ and $B_{\rho-1}(t) = B_{\rho-1}(1)$ for all $\rho < \sigma$. For $i \in B_{\sigma-1}(1)$, we have

$$X_i(t, \sigma) \geq \frac{(1 + \beta)X_i(t-1, \sigma)}{2np + \beta X_i(t-1, \sigma)}$$

For $j \in B \setminus B_{\sigma-1}(1)$,

$$X_j(t, \sigma) \leq \frac{X_j(t-1, \sigma) + (e^{6\beta \ln n} - 1)(X_j(t-1, \sigma) - 2kp - \sqrt{6kp \ln \frac{n}{k}})}{2np + (e^{6\beta \ln n} - 1)(X_j(t-1, \sigma) - 2kp - \sqrt{6kp \ln \frac{n}{k}})}$$

For

$$\beta \leq \frac{\ln \frac{n}{kL} - \frac{1}{3}}{2(\max\{\Delta p, 6 \ln n\})^2} \leq \frac{(1 - \sqrt{\frac{\Delta \ln n}{k \ln \frac{n}{k}}})^2 \ln \frac{n}{k} - \ln L - \frac{1}{3}}{2(\max\{\Delta p, 6 \ln n\})^2}$$

and $\Delta \leq k / \ln^2 n$, we have $X_j(t, \sigma) \leq X_i(t, \sigma)$ and hence, $B_{\sigma-1}(t) = B_{\sigma-1}(1)$.

Now, we will prove the last claim. For $\sigma = 1$, the argument is the same as during training since S_1 still fires, so we have $\hat{A}_\sigma = A_\sigma(1)$. Suppose that $|\hat{A}_{\sigma-1} \cap A_{\sigma-1}(1)| = (1 - \epsilon)k$. Then for $i \in A_\sigma(1)$,

$$X_i(\sigma) \geq \frac{(1 - \epsilon)(1 + \beta)^T(kp + \sqrt{\frac{3}{2}kp \ln \frac{n}{k}}) + \epsilon kp}{((1 + \beta)^T - 1)(kp + \sqrt{3kp \ln \frac{n}{k}}) + 2np} = \tau_\epsilon$$

while for $j \notin A_\sigma(1)$,

$$X_j(\sigma) \sim \frac{\mathcal{B}(k, p)}{2np}$$

Hence,

$$\begin{aligned} \Pr[j \in \hat{A}_\sigma \mid j \notin A_\sigma(1)] &\leq \Pr[X_j(\sigma) \geq \tau_\epsilon] \\ &\leq \exp \left(-\frac{1}{3kp} \left((1 - \epsilon)\beta T(kp + \sqrt{\frac{3}{2}kp \ln \frac{n}{k}}) + (1 - \epsilon)\sqrt{\frac{3}{2}kp \ln \frac{n}{k}} \right)^2 \right) \\ &\leq \exp \left(-\frac{1}{2}(1 - 2\epsilon)(1 + 2\beta T)^2 \ln \frac{n}{k} \right) \end{aligned}$$

The fraction of newcomers is hence, in expectation, no more than

$$\frac{n}{k} \exp \left(-\frac{1}{2}(1-2\epsilon)(1+2\beta T)^2 \ln \frac{n}{k} \right)$$

We seek a fixed point ϵ^* of this function. By Lemma 12, we have

$$\epsilon^* \leq \left(\frac{k}{n} \right)^{2\beta T}$$

as long as

$$T \geq \frac{1}{\beta \ln \frac{n}{k}}$$

Now, for perfect recall, suppose that

$$T \geq \frac{1}{\beta} \sqrt{\frac{\ln nL}{2 \ln \frac{n}{k}}}$$

Then

$$\exp \left(-\frac{1}{2}(1+2\beta T)^2 \ln \frac{n}{k} \right) \leq \frac{1}{nL}$$

Then a union bound over vertices and $1 \leq \sigma \leq L$ shows that the probability $\hat{A}_\sigma \neq A_\sigma(1)$ for some σ is $o(1)$. \blacksquare

Proof [Proof of Theorem 4] We first bound the overlap of the arc assemblies associated with different transitions. We then show that after sufficiently many presentations of each transitions, the connections between pairs of state and symbol assemblies and their associated arc assemblies, and between arc assemblies and the correct next state assemblies, will be sufficiently strengthened so that firing any state/symbol pair will cause the appropriate arc assembly, and then in turn the appropriate next state assembly, to fire in their entirety. Once this property is established for every transition, it follows immediately that the FSM can be simulated on an arbitrary input string.

Let $A_{q,\sigma} \subseteq A$ denote the set of neurons which fires in response to $S_q \cup I_\sigma$. We need to show that after T training presentations, if S_q and I_σ fire, then $S_{\delta(q,\sigma)}$ will fire two time steps later w.p. $1 - o(|Q|^{-1}|\Sigma|^{-1})$.

We will first bound the overlap of the sets $A_{q,\sigma}$. Suppose that $(q, \sigma) \neq (q', \sigma')$. Then

$$|(S_q \cup I_\sigma) \cap (S_{q'} \cup I_{\sigma'})| \leq k + \Delta$$

With $\Delta = o(k)$, by Lemma 11 we have $|A_{q,\sigma} \cap A_{q',\sigma'}| \leq k/2$ w.p. at least $1 - o(n^2)$. Then a union bound over all $O(|Q||\Sigma|) = O(n)$ pairs $(q, \sigma) \neq (q', \sigma')$ shows that the bound holds for every pair w.p. $1 - o(1)$.

Now, after training, it is clear that $A_{q,\sigma}$ will fire in response to S_q and I_σ . It remains to ensure that all of $S_{\delta(q,\sigma)}$ will fire. With probability $1 - o(1)$, we have

$$e(A_{q,\sigma}, i) \geq kp - \sqrt{2kp \ln n}$$

for all $i \in S_{\delta(q,\sigma)}$ and $q \in Q, \sigma \in \Sigma$. On the other hand, for any $j \in S$,

$$e(A_{q,\sigma} \cap A_{q',\sigma'}, j) \leq \frac{kp}{2} + \sqrt{\frac{3}{2}kp \ln n}$$

Let

$$X_j = e(A_{q,\sigma} \setminus A_{q',\sigma'}, j)$$

and note that X_j is the sum of i.i.d. Bernoulli random variables with $\mathbb{E}X_j \leq kp/2$. Let $S'_{q,\sigma}$ denote the cap which fires in response to $A_{q,\sigma}$. Then

$$\begin{aligned} \Pr(j \in S'_{q,\sigma} \mid j \notin S_{\delta(q,\sigma)}) &\leq \Pr\left(X_j \geq (1 + \beta)^T \left(\frac{kp}{2} - \sqrt{\frac{7}{2}kp \ln n}\right)\right) \\ &\leq \exp\left(-\frac{2(T\beta\frac{kp}{2} - (1 + T\beta)\sqrt{\frac{7}{2}kp \ln n})^2}{3kp}\right) \end{aligned}$$

For

$$T \geq \frac{12}{\beta} \sqrt{\frac{\ln n}{kp}}$$

we have

$$\Pr(j \in S'_{q,\sigma} \mid j \notin S_{\delta(q,\sigma)}) \leq \frac{1}{n^2}$$

and hence via a union bound we will have $S'_{q,\sigma} = S_{\delta(q,\sigma)}$ for every $q \in Q, \sigma \in \Sigma$ w.p. $1 - o(1)$. ■

Proof [Proof of Lemma 6] Suppose the content of the tape after L operations is $\sigma_1, \dots, \sigma_{\tilde{L}}$. We will show that with probability $1 - o(1)$, a set $A_1, \dots, A_{\tilde{L}}$ of assemblies will be created, where $A_1 \subseteq H_i$ and $A_t \subseteq H_{i+t \pmod{3}}$. This set has the properties that for any $1 \leq t \leq \tilde{L}$, (i) if A_t fires then S_{σ_t} will fire on the next round, and (ii) if A_t fires and $H_{i+t+1 \pmod{3}}$ is disinhibited then A_{t+1} will fire on the next round.

We proceed by induction on L , the number of operations. Immediately, if the $(L+1)$ th operation is “delete”, then after T rounds $H_{i+1 \pmod{3}}$ will be disinhibited, and by the inductive hypothesis then $A_2, \dots, A_{\tilde{L}}$ is a set of assemblies with the required property. So, we consider only “add” operations henceforth. We will show that each “add” operation creates an assembly A' which will fire A_1 and the associated symbol assembly with probability $1 - o(L^{-1})$. As there are at most L operations, a union bound over all operations will show the entire sequence succeeds w.p. $1 - o(1)$.

For the first “add” operation, there is no next symbol, so the set of neurons A_1 which fires randomly only needs to be linked to the correct symbol, S_{σ_1} . By Theorem 3 of Papadimitriou and Vempala (2019), for $\beta \geq \sqrt{\ln n / kp}$ A_1 will stabilize after Z_1 fires at least

$$T' = \frac{1}{\beta} \frac{\ln k}{\sqrt{kp}}$$

times. Every neuron in S_{σ_1} will have at least $kp - \sqrt{2kp \ln n}$ connections from A_1 , while no neuron outside has more than $kp + \sqrt{3kp \ln n}$. Hence, it suffices that

$$(1 + \beta)^{T-T'} \left(kp - \sqrt{2kp \ln n}\right) \geq kp + \sqrt{3kp \ln n}$$

For

$$T \geq 5 \frac{\sqrt{\ln n}}{\beta}$$

this bound holds.

Now, suppose that the first t operations were successfully simulated, for $t \geq 1$. Hence, on rounds $tT, tT + 1, \dots, tT + T - 1$, some area (say H_i) fired, while C_{delete} will fire on round $tT + T - 1$. For a “delete” operation, this implies immediately that H_{i+1} will begin to fire on round $(t + 1)T$ and continue firing through round $(t + 1)T + T - 1$. Moreover, to ensure that the correct set of neurons fires (say $A_{t+1} \subset H_{i+1}$) on round $(t + 1)T$, we need that every neuron of A_{t+1} receives more input than every neuron in $H_{i+1} \setminus A_{t+1}$. Once again, $T \geq k + 10/\beta$ will ensure this holds. Assuming A_{t+1} fires, every neuron of $S_{\sigma_{t+1}}$ has its incoming weights from A_{t+1} strengthened by $(1 + \beta)^{T - \ln k}$, so $S_{\sigma_{t+1}}$ will also fire under the same conditions on T .

On the other hand, suppose the $(t + 1)$ ’th operation adds a symbol to the beginning of the tape. By induction, some area (say H_i) fired on rounds $tT, tT + 1, \dots, (t + 1)T - 1$, while C_{add} fires on round $(t + 1)T - 1$. So, H_{i-1} will begin firing on $(t + 1)T$ (along with H_i , which will continue to fire) and continue firing until $(t + 2)T - 1$. Simultaneously, on rounds $(t + 1)T, (t + 1)T + 1, \dots, (t + 1)T + T - 1$ the assemblies $Z_{t+1}, S_{\sigma_{t+1}}$ fire together. Let A_{t+1} denote the set of neurons that fire in response to stimulus from $E_1 \cup E_2$. Then for

$$\beta T \leq \frac{\sqrt{3k} - \sqrt{36 \ln n}}{12\sqrt{\ln np}}$$

by Lemma 8 w.p. $o(L^{-1})$, we will have $|A_{t+1} \cap A_s| \leq 6 \ln n$. By Lemma 9, no neuron enters more than $6 \ln n$ assemblies.

It remains to show that the correct assembly $A_t \subseteq H_i$ will continue to fire for the next T rounds. As shown above, this will be sufficient to ensure that when A_{t+1} is firing and H_i is disinhibited, that A_t will begin firing. A neuron in A_t has fired alongside all other neurons in A_t at least T times, so its input is at least

$$(3 + \beta T) \left(kp - \sqrt{2kp \ln n} \right)$$

On the other hand any neuron outside of A_t receives at most

$$3kp + \sqrt{9kp \ln n} + 72\beta T \ln^2 n$$

input from A_{t+1}, A_t , and Z_{t+1} combined w.p. $1 - o(L^{-1})$. We then only need that

$$\beta T \left(kp - \sqrt{2kp \ln n} - 72 \ln^2 np \right) \geq \sqrt{9kp \ln n}$$

As for $kp \geq 6 \ln n$ we have

$$5 \frac{\sqrt{\ln n}}{\beta} \geq \frac{1}{\beta} \frac{\sqrt{9kp \ln n}}{kp - \sqrt{2kp \ln n} - 12 \ln^2 np}$$

this is satisfied. ■

Proof [Proof of Theorem 7] The simulation consists of three areas H_i^L, H_i^R for each of the “right” and “left” halves of the tape, a control area D for both halves of the tape jointly, and the three areas I, S, A for the FSM. The outline of its operation is as follows: The FSM simulation proceeds as in Theorem 4, modified so that if $\delta(q, \sigma) = (p, \rho, d)$, the assembly $A_{q,\sigma}$ causes S_p, I_ρ , and D_d to fire,

where $d \in \{L, R\}$. The interneurons of the FSM simulation now allow their respective areas to fire after T rounds, where T is the number of repetitions required by the tape simulation. The tape halves are configured as in Lemma 6, where the firing of D_L signals a deletion for the left half and a addition of the top symbol from the left half for the right stack. The new assembly on the right half becomes linked to I_σ by their concurrent firing, which effects a leftward movement of the tape head (and similarly for D_R).

By Theorem 4, the FSM simulation in areas I, S, A will simulate the transition function of the Turing machine w.h.p., while by Lemma 6 each of the stack simulations will perform as desired w.h.p. which simulates the TM’s tape. We then have three events which each occur w.h.p., so their intersection does as well. ■

5. Discussion

NEMO is a simple mathematical model of the brain involving random connectivity, Hebbian plasticity, local inhibition, and long-range interneurons, which provably captures key aspects of cognition involving sequences. Here we demonstrated that sequences can be memorized and copied in various modes, and furthermore that, through sequences, our model can learn to recognize patterns modeled by finite state machines; a more sophisticated use of sequences of assemblies is capable of universal computation. While this last point is of course primarily of theoretical interest, it is a rather useful point to make about the power of NEMO as a model of brain computation. Brain-like computation can happen with no explicit control flow or commands — that is to say, no *program*. All that is needed is biologically plausible neural hardware and the presentation of stimuli.

A striking difference in the behavior of the brain and silicon computers is in their mechanisms for the creation and recall of memories. This is the starting point of the assembly model, continued here. A very interesting and unexpected discovery is rigorous mathematical evidence for the emergence of the utility of mnemonics, memory palaces and other memory aids (Maguire et al., 2003), a uniquely brain-centered phenomenon that has no analogy for computers.

Although we have explored how the brain might encode and memorize sequences here, a crucial gap remains: How the brain generates sequences. Augmenting our FSM simulation with probabilistic transitions would allow it to generate random sequences, effectively capturing the brain’s ability to sample from a *probabilistic* finite automaton; this approach could be further generalized to allow sampling from a graphical model. How probabilistic transitions might be realized in NEMO, and moreover learned from streams of stimuli, is an important and urgent future direction for this work, and would be the basis of emergent statistical computation in the brain.

Finally, we must note that, in our discussion of the way in which sequences are memorized and recalled in the brain, we have not yet mentioned *language*, arguably the most remarkable faculty related to sequences that human brains enjoy; see Mitropolsky et al. (2021, 2022) for work on assemblies and language.

Acknowledgments

MD and SV are supported in part by NSF awards CCF-1909756, CCF-2007443 and CCF-2134105, and a NSF Graduate Research Fellowship. CP is supported by NSF Awards CCF-1763970 and CCF-1910700, and a research contract with Softbank.

References

- Jacob LS Bellmund, Ignacio Polti, and Christian F Doeller. Sequence memory in the hippocampal–entorhinal region. *Journal of Cognitive Neuroscience*, 32(11):2056–2070, 2020.
- György Buzsáki. Neural syntax: cell assemblies, synapsembles, and readers. *Neuron*, 68(3):362–385, 2010.
- György Buzsáki. *The Brain from Inside Out*. Oxford University Press, 2019.
- Scott J Cruikshank, Timothy J Lewis, and Barry W Connors. Synaptic basis for intense thalamocortical activation of feedforward inhibitory cells in neocortex. *Nature neuroscience*, 10(4):462–468, 2007.
- Yuwei Cui, Subutai Ahmad, and Jeff Hawkins. Continuous online sequence learning with an unsupervised neural network model. *Neural computation*, 28(11):2474–2504, 2016.
- Max Dabagia, Santosh S Vempala, and Christos Papadimitriou. Assemblies of neurons learn to classify well-separated distributions. In *Conference on Learning Theory*, pages 3685–3717. PMLR, 2022.
- George Dragoi and György Buzsáki. Temporal encoding of place sequences by hippocampal cell assemblies. *Neuron*, 50(1):145–157, 2006.
- George Dragoi and Susumu Tonegawa. Preplay of future place cell sequences by hippocampal cellular assemblies. *Nature*, 469(7330):397–401, 2011.
- Howard Eichenbaum. Barlow versus hebb: When is it time to abandon the notion of feature detectors and adopt the cell assembly as the unit of cognition? *Neuroscience letters*, 680:88–93, 2018.
- Chris Eliasmith, Terrence C Stewart, Xuan Choo, Trevor Bekolay, Travis DeWolf, Yichuan Tang, and Daniel Rasmussen. A large-scale model of the functioning brain. *science*, 338(6111):1202–1205, 2012.
- Vitaly Feldman and Leslie G Valiant. Experience-induced neural circuits that achieve high capacity. *Neural computation*, 21(10):2715–2754, 2009.
- Jordan Guerguiev, Timothy P Lillicrap, and Blake A Richards. Towards deep learning with segregated dendrites. *Elife*, 6:e22901, 2017.
- Kenneth D Harris, Jozsef Csicsvari, Hajime Hirase, George Dragoi, and György Buzsáki. Organization of cell assemblies in the hippocampus. *Nature*, 424(6948):552–556, 2003.
- Donald Olding Hebb. *The organization of behavior: A neuropsychological theory*. John Wiley, 1949.
- Christian R Huyck and Peter J Passmore. A review of cell assemblies. *Biological cybernetics*, 107: 263–288, 2013.

- Yuji Ikegaya, Gloster Aaron, Rosa Cossart, Dmitriy Aronov, Ilan Lampl, David Ferster, and Rafael Yuste. Synfire chains and cortical songs: temporal modules of cortical activity. *Science*, 304(5670):559–564, 2004.
- Shozo Jinno, Thomas Klausberger, Laszlo F Marton, Yannis Dalezios, J David B Roberts, Pablo Fuentealba, Eric A Bushong, Darrell Henze, György Buzsáki, and Peter Somogyi. Neuronal diversity in gabaergic long-range projections from the hippocampus. *Journal of Neuroscience*, 27(33):8790–8804, 2007.
- Timothy P Lillicrap, Daniel Cownden, Douglas B Tweed, and Colin J Akerman. Random synaptic feedback weights support error backpropagation for deep learning. *Nature communications*, 7(1):13276, 2016.
- Timothy P Lillicrap, Adam Santoro, Luke Marris, Colin J Akerman, and Geoffrey Hinton. Back-propagation and the brain. *Nature Reviews Neuroscience*, 21(6):335–346, 2020.
- Eleanor A Maguire, Elizabeth R Valentine, John M Wilding, and Narinder Kapur. Routes to remembering: the brains behind superior memory. *Nature neuroscience*, 6(1):90–95, 2003.
- Daniel Mitropolsky, Michael J Collins, and Christos H Papadimitriou. A biologically plausible parser. *Transactions of the Association for Computational Linguistics*, 9:1374–1388, 2021.
- Daniel Mitropolsky, Adiba Ejaz, Mirah Shi, Mihalis Yannakakis, and Christos H Papadimitriou. Center-embedding and constituency in the brain and a new characterization of context-free languages. *arXiv preprint arXiv:2206.13217*, 2022.
- Christos H Papadimitriou and Santosh S Vempala. Random projection in the brain and computation with assemblies of neurons. In *10th Innovations in Theoretical Computer Science Conference*, 2019.
- Christos H Papadimitriou, Santosh S Vempala, Daniel Mitropolsky, Michael Collins, and Wolfgang Maass. Brain computation by assemblies of neurons. *Proceedings of the National Academy of Sciences*, 117(25):14464–14472, 2020.
- Eva Pastalkova, Vladimir Itskov, Asohan Amarasingham, and Gyorgy Buzsaki. Internally generated cell assembly sequences in the rat hippocampus. *Science*, 321(5894):1322–1327, 2008.
- Lisa Roux and György Buzsáki. Tasks for inhibitory interneurons in intact brain circuits. *Neuropharmacology*, 88:10–23, 2015.
- Joao Sacramento, Rui Ponte Costa, Yoshua Bengio, and Walter Senn. Dendritic error backpropagation in deep cortical microcircuits. *arXiv preprint arXiv:1801.00062*, 2017.
- João Sacramento, Rui Ponte Costa, Yoshua Bengio, and Walter Senn. Dendritic cortical microcircuits approximate the backpropagation algorithm. *Advances in neural information processing systems*, 31, 2018.
- A Sik, M Penttonen, A Ylinen, and Gy Buzsáki. Hippocampal cal interneurons: an in vivo intracellular labeling study. *Journal of Neuroscience*, 15(10):6651–6665, 1995.

- Michael Sipser. Introduction to the theory of computation. *ACM Sigact News*, 27(1):27–29, 1996.
- Jørgen Sugar and May-Britt Moser. Episodic memory: Neuronal codes for what, where, and when. *Hippocampus*, 29(12):1190–1205, 2019.
- Leslie G Valiant. *Circuits of the Mind*. Oxford University Press on Demand, 2000a.
- Leslie G Valiant. A neuroidal architecture for cognitive computation. *Journal of the ACM (JACM)*, 47(5):854–882, 2000b.
- James CR Whittington and Rafal Bogacz. Theories of error back-propagation in the brain. *Trends in cognitive sciences*, 23(3):235–250, 2019.
- James CR Whittington, Timothy H Muller, Shirley Mark, Guifen Chen, Caswell Barry, Neil Burgess, and Timothy EJ Behrens. The tolmán-eichenbaum machine: unifying space and relational memory through generalization in the hippocampal formation. *Cell*, 183(5):1249–1263, 2020.
- Rafael Yuste. From the neuron doctrine to neural networks. *Nature reviews neuroscience*, 16(8):487–497, 2015.
- Siyu Zhang, Min Xu, Tsukasa Kamigaki, Johnny Phong Hoang Do, Wei-Cheng Chang, Sean Jenvay, Kazunari Miyamichi, Liqun Luo, and Yang Dan. Long-range and local circuits for top-down modulation of visual cortex processing. *Science*, 345(6197):660–665, 2014.
- Fu-Ming Zhou and John J Hablitz. Ampa receptor-mediated epscs in rat neocortical layer ii/iii interneurons have rapid kinetics. *Brain research*, 780(1):166–169, 1998.